Received: 20 May 2022 | Revised: 24 November 2022 | Accepted: 27 December 2022 | Published on: 24 January 2023

DOI: 10.1002/joc.8002

RESEARCH ARTICLE

International Journal of Climatology RMetS

Diverging snowfall trends across months and elevation in the northeastern Italian Alps

Giacomo Bertoldi[1] | Michele Bozzoli[1,2] | Alice Crespi[3] | Michael Matiu[2,3] | Lorenzo Giovannini[2] | Dino Zardi[2] | Bruno Majone[2]

[1]Institute for Alpine Environment, Eurac Research, Bolzano, Italy

[2]Department of Civil, Environmental and Mechanical Engineering, University of Trento, Trento, Italy

[3]Institute for Earth Observation, Eurac Research, Bolzano, Italy

Correspondence
Giacomo Bertoldi, Institute for Alpine Environment, Eurac Research, Bolzano, BZ, 39100, Italy.
Email: giacomo.bertoldi@eurac.edu

Funding information
Eurac Research, Grant/Award Number: Ecohydro; Autonomous Province of Bozen/Bolzano; SHE – Seasonal Hydrological-Econometric forecasting for hydropower optimization; SnowTinel: Sentinel-1 SAR assisted catchment hydrology: toward an improved snow-melt dynamics for alpine regions

Abstract

Snowfall and snow accumulation play a crucial role in shaping ecosystems and human activities in the Alpine region. This resource is under threat as a consequence of the visible effects of global warming, and, therefore, it appears urgent to understand how snowfall trends have changed in time and space. In this context, we recovered data from over a hundred snowfall (HN) time series covering the period 1980–2020 over the mountain region of Trentino-South Tyrol in the northeastern Italian Alps and analysed them to understand snowfall climatology in the region, recent trends and their dependence on elevation and timing of the season. Negative, although not always statistically significant, trends were found in the lowest elevation range (0–1,000 m a.s.l.) over the whole winter season, while some positive and even significant trends were found from January to March above 2,000 m a.s.l. The intermediate elevation range (1,000–2,000 m a.s.l.) exhibits a strong variability with no clear trend. Negative and statistically significant trends were found in April for all elevations. An attribution analysis was performed using precipitation (P), mean air temperature (TMEAN), and large-scale synoptic descriptors, such as the North Atlantic Oscillation (NAO) and the Arctic Oscillation (AO) indices. The analysis shows that, overall, P is the driver that best explains the snowfall trends, but, for low elevations, especially during mid-winter, TMEAN is more relevant. Low elevations are facing a clear decrease in HN due to a significant increase in mean temperatures, while high elevations during mid-winter display a slight increase in HN, associated with a general increase in precipitation. NAO and AO indices exhibit no significant correlations with HN, except at the lowest elevations and at the beginning of the season.

KEYWORDS

Alps, attribution, climatology, snowfall, trends

1 | INTRODUCTION

Snow is a key component of the water cycle in mountain watersheds, controlling timing and magnitude of runoff generation processes (Majone *et al.*, 2016; Marke *et al.*, 2018; Di Marco *et al.*, 2021). Snow contributes to the seasonal storage of water that becomes available later trough snowmelt, for agricultural, civil and industrial uses. Moreover, snow plays an important role in shaping the natural environment of mountain regions, affecting the vegetation cycle, mountain flora and fauna, biodiversity and related ecosystem services (Keller *et al.*, 2005). Snow cover is also one of the key elements of the Earth's energy budget, since it strongly affects the surface heat and radiation balance, significantly influencing near-surface air temperature (Jin and Miller, 2007). Finally, the presence and availability of snow are the fundamental prerequisites for many economic and recreational activities, as, for instance, hydropower production (Majone *et al.*, 2016) and winter mountain tourism (Olefs *et al.*, 2020).

Considering current threats posed by climate change on the cryosphere (Frei *et al.*, 2017; Huss *et al.*, 2017; Mote *et al.*, 2018; Kotlarski *et al.*, 2022), it is urgent to recover historical snow observations to understand how snowfall trends have been changing over time. During the past decades, a decreasing trend has been detected from reanalyses for both snowfall amounts and snowfall days over most regions of Eurasia (Lin and Chen, 2022). Over northern Eurasia, Ye and Cohen (2013) found a mean decrease in the duration of the snowfall season of 6.2 days per 1°C of temperature increase, split between the start (−2.8 days) and end of the season (−3.4 days). The frequency of daily snowfall events is projected to further decrease across much of the Northern Hemisphere, except at the highest latitudes such as in northern Canada, northern Siberia and Greenland (Danco *et al.*, 2016).

Snow and snow cover can be quantified using different parameters. The most commonly used are snow depth (HS), depth of fresh snow precipitation (HN, also denoted as snowfall), snow water equivalent (SWE), snow cover area (SCA) and snow cover duration (SCD) (see, e.g., Pirazzini *et al.*, 2018; Haberkorn, 2019). Almost all the studies available in the literature are focused on HS, SWE or SCD, while limited attention has been given to snowfall (HN). However, it is important to recover HN observations, understand its change over time and compare HN with liquid precipitation trends, as HN and the solid–liquid precipitation ratio are very sensitive to climate change (Guo and Li, 2015). Moreover, since snowfall is a solid precipitation, it is more easily compared with the liquid precipitation than with the snow depth. Therefore, the comparison of snowfall trends with those of liquid precipitation and mean air temperature is essential to better understand which of these two drivers plays a more important role, depending on elevation and local climate, especially in mountain regions.

The detected general decrease of snow over the Alps in the last decades is projected to continue during the 21st century on the basis of the available climate change scenarios (Kotlarski *et al.*, 2022). Superimposed on the long-term trend, however, there is a low-frequency variability of snowfall associated with multidecadal changes in the large-scale circulation. In fact, the leading mode of wintertime atmospheric variability over the North Atlantic-North Eurasia sector is dominated by the the Arctic Oscillation (AO) and the North Atlantic Oscillation (NAO), with this latter found to contribute significantly to recent trends in surface air temperature, snowfall, snow water equivalent and snow cover over Eurasia (Ye *et al.*, 2022). For those reasons, in order to understand the major climatic drivers responsible for snowfall trends in the Alpine region, besides considering surface variables as precipitation and temperature, it is important to take into account large-scale indices as NAO and AO.

In recent years, several efforts have been made to build reliable snow climatologies worldwide, including mountain regions, where orography strongly influences temperature and precipitation gradients and therefore snowfall climatology exhibits complex spatial patterns (Beniston *et al.*, 2018; Pepin *et al.*, 2022). In this respect, remote sensing (Hammond *et al.*, 2018) and climate model reanalyses (Olefs *et al.*, 2020; Li *et al.*, 2021) can provide reliable spatially distributed data, but with some limitations. In fact, on one hand, remote sensing can provide high-resolution information on snow covered area only after 2000 with the introduction of the MODIS constellation (Notarnicola, 2020; Fugazza *et al.*, 2021). On the other hand, reanalyses may suffer from accuracy limitations (Vernay *et al.*, 2022), mainly due to the low spatial resolution and to the poor representation of subgrid processes (e.g., convection and associated precipitation, thermal inversion in mountain valleys controlling snowfall line). Both issues are particularly relevant in regions characterized by complex terrain (Kotlarski *et al.*, 2014). In this context, it is evident that reliable identification of long-term snow trends should still mostly rely on long and accurate time series of ground observations. On the other hand, high-quality ground observations could serve for validating remote sensing and modelled snow products. Furthermore, detailed analyses of snowfall data are required to better constrain and quantify climate change impacts in mountain regions and their relation to elevation (Beaumet *et al.*, 2021), whereby understanding how warming rates are stratified by elevation, which is still a current open research question (Pepin *et al.*, 2022).

Focusing on the European Alps, a large number of snow-recording stations, operated by different

authorities, some of them dating back to the late 18th century (Leporati and Mercalli, 1994), allow to draw a general picture of current snow trends. At the European scale, it has been observed that SCD during the period 1972–2006 was related to large scale atmospheric patterns, in particular it was strongly connected to AO observed during wintertime (Bartolini *et al*., 2010). Concerning SWE, a significant decrease has been noticed during the last six decades, more pronounced during spring than during winter, and quite independent from latitude and longitude (Marty *et al*., 2017). Also for snow depth, decreasing trends have been observed for the entire Alpine region by Matiu *et al*. (2021), who evaluated linear trends of mean monthly HS between 1971 and 2019 and concluded that 87% of the stations analysed are characterized by a decrease in snow depth, with stronger negative trends from March to May than from December to February.

At a regional scale, different studies were also performed taking advantage of databases from national monitoring networks. In particular, Marke *et al*. (2018) performed a comparison of SCD in different sub-regions of Austria during the periods 1950–1979 and 1980–2009, highlighting a general decreasing trend with mean changes between −11 and −15 days. Olefs *et al*. (2017) and Olefs *et al*. (2020) confirmed a negative trend for SCD, though not strongly related to elevation. In the Swiss Alps, Scherrer *et al*. (2013) calculated snow climate indicators such as new snow sums (NSS), maximum new snow (MAXNS) and days with snowfall (DWSF) and analysed their variability and trends. Looking at NSS, MAXNS and DWSF, they found a large decadal variability with phases of low and high values and the lowest values and unprecedented negative trends in the late 1980s and 1990s. This was confirmed also by Marty (2008). Analysing the number of days with snow cover from 34 long-term stations between 200 and 1,800 m a.s.l., he found an unprecedented series of low snow winters in the last 20 years. In a more recent study, Marty and Blanchet (2012), using snowfall data from 25 stations (between 200 and 2,500 m a.s.l.) collected during the last 80 winters (1930/1931 to 2009/2010), discovered that all the stations, even the highest one, showed a decrease in extreme snow depth, which was mainly significant at low altitudes (below 800 m a.s.l.). A negative trend was also observed for extreme snowfalls at low and high altitudes, but the pattern at mid-altitudes (between 800 and 1,500 m a.s.l.) was less clear.

In France, Durand *et al*. (2009) analysed snow data from the Crocus snow model driven by reanalyses in the period 1958–2005, highlighting that snow patterns are characterized by a marked declining trend from the northwestern foothills to the southeastern interior regions. This situation applies mainly to both HS and SCD, which exhibits a maximum variation at 1,500 m a.s.l. of about 60 days, decreasing strongly with elevation. Moreover, they noticed that SCD shows a significant general signal of decrease at low and mid elevations, but this signal is weaker in the southern than in the northern France, and less visible at high elevation.

Finally, studies on snow trends are also available for northern Italy, although covering a limited spatial extent. Valt and Cianfarra (2010) highlighted the presence of breakpoints between 1984 and 1994. These breakpoints mark a drastic change of trend in the time series: a positive trend characterizes the time series before the breakpoint and a decreasing trend characterizes the historical record after the breakpoint. In particular, stronger negative trends below 1,500 m a.s.l. were found during springtime, associated with a precipitation decrease. In Piedmont, the analysis of six long-term snow depth stations located between 960 and 2,177 m a.s.l. highlighted a significant decrease of snow depth in the period 1951–2010, with the main contribution from spring months (Terzago *et al*., 2013). In the Adige catchment (Trentino-South Tyrol, northeastern Italy) Marcolini *et al*. (2017) analysed data of mean seasonal snow depth and SCD collected in the period 1980–2009, showing that different dynamics can be observed above and below 1,650 m a.s.l., with a large reduction of average snow depth and SCD for stations below that elevation.

For the Italian Alps, numerous (300+) HN daily series have been recently collected by Matiu *et al*. (2020), covering several decades, mainly from measurements performed by local institutions in mountain ski resorts for avalanche prevention purposes. However, observations are scarce, both at high elevations, where observations are more complex, and at low elevations, where snowfall is less frequent, but more affected by climatic variability. In the last years, amateur observation networks, managed by individuals with great competence and passion, are increasingly contributing to complement official meteorological observation networks (Endfield and Morris, 2012; Wolters and Brandsma, 2012; Mateus, 2021). However, to our knowledge, such HN observations have never been exploited so far, at least for scientific climatological purposes.

The first objective of this study is to collect and analyse snowfall data of the northeastern Italian Alps during wintertime, coming from both official and amateur observations. The second objective is to analyse snowfall trends and compare them with those of snow depth, retrieved from Matiu *et al*. (2021). Another important purpose of this study is to understand what are the main factors influencing snowfall and its trend, depending on the elevation. We select four different drivers: precipitation (P),

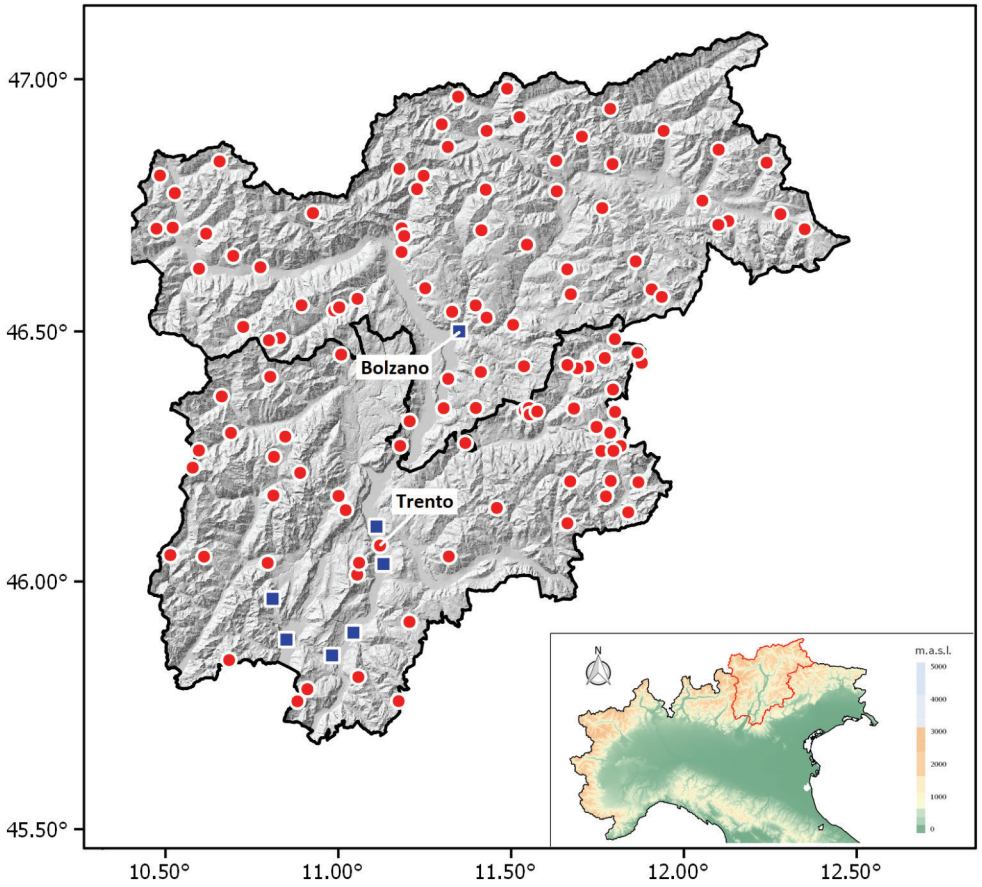

FIGURE 1 The study region of Trentino-South Tyrol with institutional (red circles) and amateur (blue squares) snow stations. The lower right inset shows the location of the study region in the Italian territory [Colour figure can be viewed at wileyonlinelibrary.com]

mean air temperature (TMEAN), North Atlantic Oscillation (NAO) and Arctic Oscillation (AO) indices. The first two are self-explanatory, as HN is directly influenced by both P and TMEAN. The other two are taken into consideration to evaluate if HN can be related to some indices of large-scale circulation patterns, as suggested for example by Quadrelli *et al*. (2001). Therefore, we conduct a so-called "driver attribution" analysis, in order to better understand which driver among P, TMEAN, NAO and AO plays a more relevant role to explain HN variability.

The paper is structured as follows: sections 2 and 3 describe all the preliminary operations done to prepare the database and the techniques used to evaluate statistics and trends. Section 4 provides results and section 5 discusses them. Finally, section 6 summarizes the results and draws some conclusions.

2 | STUDY AREA AND AVAILABLE DATA

The Trentino-South Tyrol region is located in the north-eastern part of the Italian Alps. Its territory is mainly mountainous, with a mean elevation of 1,600 m a.s.l. (Figure 1). Elevations range from 65 to 3,900 m a.s.l., determining a strong local climatic variability. Valley floors typically experience warmer temperatures than mountainous areas, but with a much more pronounced annual temperature amplitude, with hot summers, but also low temperatures in winter, especially for the frequent occurrence of ground based thermal inversions, associated with reduced incoming solar radiation. High-elevation areas, on the other hand, experience colder temperatures and a smaller seasonal temperature range. Precipitation is influenced by orography, with higher values in the mountainous areas than in the valleys, especially over the mountain chains well exposed to southern moist airflows (see, e.g., Laiti *et al*., 2018). Precipitation is mainly concentrated in autumn and spring in the southern part of the region, while the regime is more continental in the northern part, close to the main Alpine divide, where maximum precipitations are experienced in summer (Brunetti *et al*., 2006). A comprehensive overview of the regional climate can be found in Chiogna *et al*. (2016) and Adler *et al*. (2015).

2.1 | Data

The HN database exploited in this study is composed of 122 time series from long-term snow monitoring stations in the Trentino-South Tyrol region (Figure 1). Most of

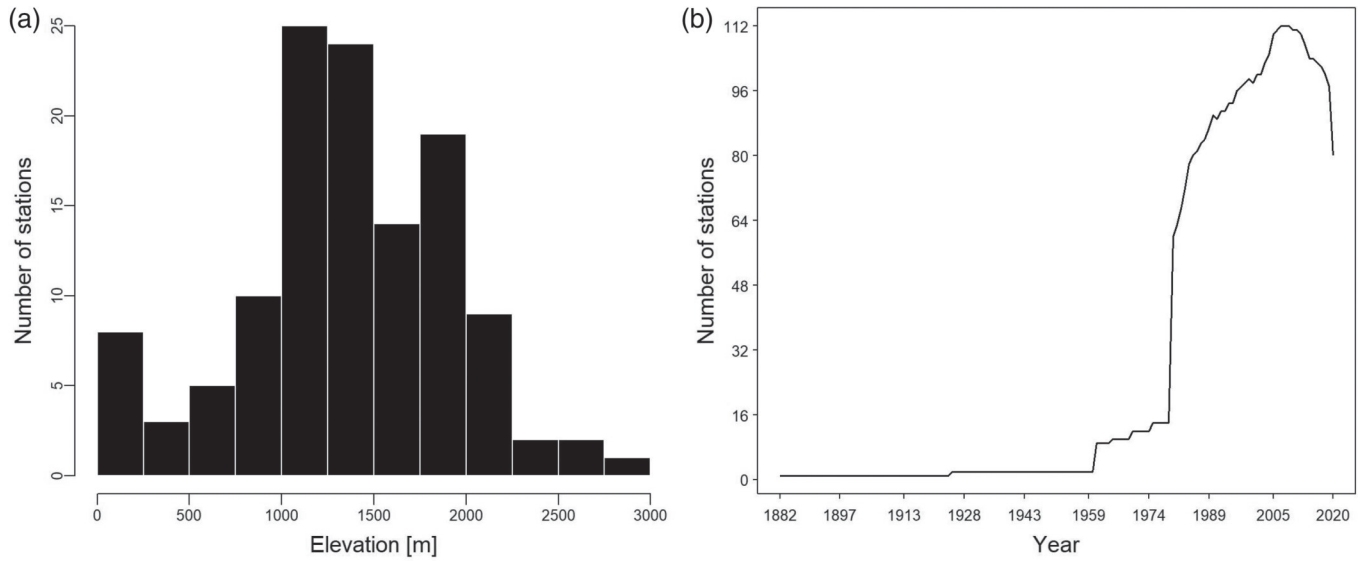

FIGURE 2 Number of available stations per elevation (a) and year (b)

the information was retrieved from the Alpine-wide observation database set up by Matiu *et al.* (2021). Specifically, we considered 115 series of daily HN observations provided by the Meteorological Services of the Provinces of Bolzano and Trento (red dots in Figure 1). These data had already been preliminary quality-checked for detecting possible macroscopic wrong recordings (e.g., negative values of HN), but no detailed quality check had been performed before this work. For the present study, the database was integrated with 7 HN time series at monthly resolution, provided by the amateur association "Meteo Trentino-Alto Adige" (MTTA), which allowed to increase the data coverage below 1,000 m a.s.l., especially in the Province of Trento (blue squares in Figure 1). The official observations were collected by following the MOD1 AINEVA protocol (https://content.meteotrentino.it/neve-ghiacci/Husky/mod1/legenda-mod1.pdf), which requires a daily measurement of the snowfall over a wooden table in the early morning hours, generally between 0700 and 0900 LST (UTC+1). Instead, the amateur stations measured the total snow accumulated at the end of the event on an empty and clean surface, a wooden table or short grass. If the event lasted several days, a measurement was taken once a day to mark the daily accumulation, with the exception of Riva del Garda and Rovereto stations (see Figure 4a for the exact location), where measurements were taken three times a day, approximately every 7 hr. At these two stations the daily total was calculated as the sum of the three measurements taken during the day. Following Helfricht *et al.* (2018), Anderson's equation (Anderson, 1976) was used to estimate the measurement error due to snow settlement, which resulted in a maximum daily error of about 10% for standard snowfall rates (precipitation intensity less than 5 $mm \cdot hr^{-1}$) and air temperature below 0°C. This error is acceptable and in line with the one mentioned for the official networks. For more detailed information on the measuring procedures, we refer to the European Snow Booklet (Haberkorn, 2019). Values of HN were rounded to full centimetres.

The spatial distribution of HN stations is quite uniform over the entire region, as shown in Figure 1. In terms of elevation distribution, most of the sites (82) are located between 1,000 and 2,000 m a.s.l., 26 are below 1,000 m a.s.l., and 14 are above 2,000 m a.s.l. (Figure 2a). Thanks to the technological development and the transition of the nivological monitoring competences to the autonomous provinces of Trentino and South Tyrol, the number of available stations strongly increased after 1980 (Figure 2b).

In order to better discuss and interpret HN trends, the monthly records of total snow depth (HS) for the same sites and time period, except for the MTTA ones, were also considered. HS data were extracted from the quality-checked and gap-filled HS database released by Matiu *et al.* (2020). All the applied quality controls and data validation criteria for HS are described in detail by Matiu *et al.* (2021).

Furthermore, monthly time series of total precipitation (P) and mean temperature (TMEAN) at each site were also retrieved, in order to perform a formal attribution analysis. Most of the snow stations are located near temperature stations, but many of them do not include liquid precipitation observations. To overcome this problem, the TMEAN and P series were extracted from the grid cell closest to the snow station location, as provided by the high-resolution 250-m gridded observational database for Trentino-South Tyrol produced by Crespi *et al.* (2021) and covering the period 1980–2018. The database

was created starting from an archive of daily observation time series from more than 200 meteorological stations by means of an anomaly-based interpolation scheme. Crespi *et al.* (2021) report an accuracy for the daily records, evaluated in terms of mean absolute error (MAE), of about 1.5°C for TMEAN and 1.1 mm for P fields. The spatial resolution of this database is accurate enough to consider as negligible the errors attributable to the difference between station locations and grid points. The database provided by Crespi *et al.* (2021) was also updated to 2020 in order to extend the comparison over the entire period spanned by HN data. As further potential drivers of HN variability, the 1980–2020 monthly series of NAO and AO were retrieved from the National Oceanic and Atmospheric Administration (NOAA) website (https://psl.noaa.gov/data/climateindices/list). These indices are called "teleconnection indices" and are used as descriptive parameters of the synoptic conditions that can occur over Europe, especially from autumn to spring (Bartolini *et al.*, 2010; Capozzi *et al.*, 2021). We selected NAO and AO since those indices explain most of the Alpine precipitation variance (Quadrelli *et al.*, 2001).

3 | METHODS

3.1 | Data processing

Since the aim of the present study is to analyse long-term snowfall (HN) trends over Trentino-South Tyrol on a monthly and seasonal scale, all daily data retrieved from Matiu *et al.* (2021) were converted into monthly series by computing the total HN accumulated over each month. In order to avoid underestimations of monthly totals due to missing daily records, monthly aggregations were computed only if less than 30% of daily values in the month were missing. This threshold was defined in order to minimize the fraction of missing monthly values and, at the same time, to ensure the reliability of the aggregation procedure. The analysis covers the period 1980–2020, which corresponds to the years with the highest data availability (Figure 2b). In fact, most of the collected series start after 1980 and only 15 sites include records covering earlier decades. After aggregating at the monthly time scale, data were subjected to a quality check to assess spatial and temporal consistency. Furthermore, a gap-filling procedure was implemented for maximizing the data availability.

3.2 | Data quality check and gap filling

The spatial and temporal consistency of the database were evaluated following a scheme similar to the one proposed by Matiu *et al.* (2021) for the snow depth (HS). This procedure is able to reconstruct monthly values of a station (test station) through an average of the records available from up to 10 neighbouring stations (reference stations). The reference stations are selected using a proximity criteria in which horizontal and vertical distances from the test station are weighted differently. Weights are evaluated using an exponential decay ("half-time" transformation of decay constant). In the case of Matiu *et al.* (2021), this implies that the weights are halved every 200 km and 500 m for the horizontal and vertical distances, respectively. Only stations including available data for the considered month, and covering at least 10 years of data in common with the site under reconstruction are considered as reference. Each reference value is re-scaled by the ratio of test and reference mean HN for the considered month and the final prediction value is defined as the average of all the values reconstructed by using the reference stations. Different tests were performed changing the previous parameters in order to assess the sensitivity. However, since our study area is smaller than that of Matiu *et al.* (2021) and HN time series are much more discontinuous, the best solution was found setting 20 km and 200 m for the horizontal and vertical distance halving coefficients, respectively, and 10 years as the minimum number of common years between test and reference stations.

The quality check of the data was thus performed by applying this procedure to the monthly HN time series of each observation site. Each simulated series was then compared with the observed one and the agreement was evaluated in terms of mean error (BIAS), mean absolute error (MAE), in both absolute and relative terms, and squared correlation (R^2). Relative errors were calculated with respect to the monthly average HN of each time series. To identify possible erroneous series, we looked at the error distributions (see Figure A1 of Appendix A). We then derived the following thresholds, which separate the main from marginal errors: 4% for the relative BIAS, 45% for the relative MAE, or below 0.5 for R^2. The aim here is not to find an automatic procedure to remove stations, but to identify the cases with the lowest agreement between observed and simulated values. The stations outside these thresholds were further checked manually. From these, only one obvious outlier in February 2014 for Cortaccia (South Tyrol) station was detected and removed. The average reconstruction BIAS, MAE and R^2 over all sites were 0.6 cm (1.5%), 12.1 cm (32.4%) and 0.74, respectively.

After the quality check, the same procedure was used for gap filling to reconstruct missing monthly entries of all HN series. Considering only the months analysed, that is, from October to April, 53% of the total monthly data

were missing. After the gap filling, this percentage was reduced to 27%. However, a portion of missing values at the beginning and at the end of the snow season was not reconstructed, especially for the Province of Trento, since many stations are not active in these months, as no important snow events are expected. Moreover, a sensitivity analysis has been performed to better understand how much the resulting trends were affected by the gap filling procedure. It was decided to discard the time series where the gap filling data gain was above a certain threshold. The thresholds imposed on the % of data gained thanks to the gap filling procedure were 10, 20, and 30%. In Figures B1–B3 and Table B1 of Appendix B, all the three different test cases and a comparative table of trends are reported. It can be seen that, besides the reduction in the stations number, the trends pattern is the same as the one obtained using no thresholds (see Figure 5). Also, looking at the trend values, not much differences can be seen, except for the stations in the highest elevation band, which are too few (only 5) to make a robust trend estimation. Therefore, it was decided to keep the full set to get a better spatial cover.

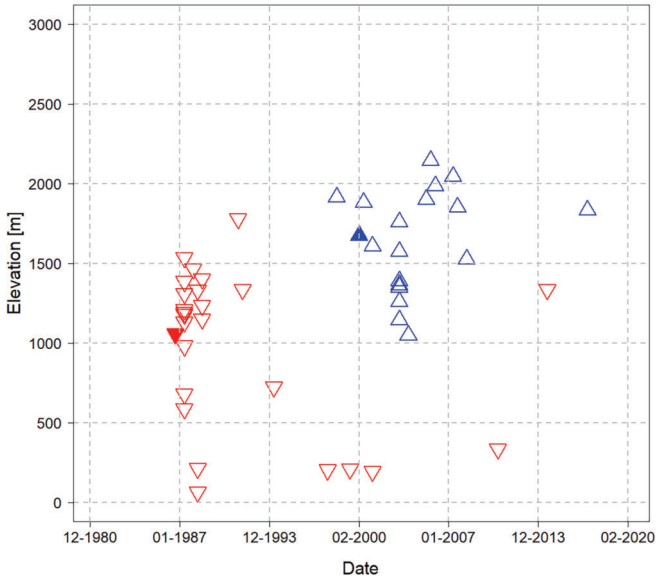

FIGURE 3 Time series changing points as function of elevation. Each point represents one station. Blue (red) triangles indicate positive (negative) changing points. Full triangles indicate significant changing points [Colour figure can be viewed at wileyonlinelibrary.com]

3.3 | Temporal homogeneity check

The assessment of homogeneity of climate series represents a crucial aspect when long-term trends are analysed. While several homogeneity tests have been developed and are a common practice for temperature and precipitation series, only a few studies discussed and addressed the homogenization of snow series (Marcolini *et al.*, 2017; Marcolini *et al.*, 2019; Schöner *et al.*, 2019; Buchmann *et al.*, 2021; Buchmann *et al.*, 2022). However, due to the relative short temporal extent of the HN series analysed here, and the lack of homogeneous series to be used as reference, no systematic test for homogeneity assessment and series homogenization was applied to the HN database. Nevertheless, the procedure for analysing the spatial and temporal consistency previously described did not highlight suspicious deviations and drifts with respect to nearby observations for any site. In addition, a change-point detection analysis based on the Pettitt's test (Pettitt, 1979) was performed for all time series. The test was implemented considering the period from December to February, due to the more limited data availability in autumn and spring. Figure 3 shows that the Pettitt's test detected only two significant changing points: December 1986 for "Diga_di_Valdaora_Osservatore" in the northeastern part of the Bolzano province and February 2000 for "Predazzo_gardone" in the northeastern part of the Trento province. Changing points for all sites above 1,000 m a.s.l. mostly occurred in two periods: in the late 1980s and from 2000 to 2008 (Figure 3). The breakpoints at the end of the 1980s are all negative and represent a climate anomaly, as supported by the conclusions reported in several studies performed in the region (Durand *et al.*, 2009; Valt and Cianfarra, 2010; Mallucci *et al.*, 2019) and also at global level (Reid *et al.*, 2016). Instead, the changing points in the 2000s are mostly positive, indicating a possible phase of increasing snowfall, especially for mid–high altitudes (see section 5 for further considerations). Therefore, there is no evidence of relevant inhomogeneities in the HN time series, which have been then used in this work to detect long-term trends.

3.4 | Statistical analyses

Different statistical tests were performed to detect, assess and attribute snowfall long-term trends. To evaluate trends significance over time, the Mann–Kendall (MK) trend test (Mann, 1945; Kendall, 1975) was used. MK tests for a monotonic upward (or downward) trend, which indicates that the variable consistently increases (or decreases) over time, no matter if the trend is linear or nonlinear. In this work, statistical significance implies a *p*-value less than .05, unless otherwise stated. For assessing the trend magnitudes the nonparametric procedure developed by Sen (1968) was used, which estimates the trend slope in the sample of all *N* data pairs. The value of the median

of all the slopes evaluated for each data pair reflects the overall steepness of the trend. Sen's slope is a nonparametric alternative to trend evaluation by means of ordinary least squares, and it is considered as a robust estimator, particularly in the case of nonlinear trends. Mean values of the absolute and relative trends were computed for three different elevation ranges: (0, 1000], (1000, 2000] and (2000, 3000] m, that will be hereafter termed as "low", "medium" and "high" altitudes, respectively.

To measure the bi-variate relationship between time series of variables (HN vs. P, TMEAN, NAO and AO), the Pearson correlation coefficient was used, which is based on the evaluation of covariance between two variables (Freedman *et al*., 2007). It provides information about the magnitude of the linear association, as well as the sign of the relationship. The stronger the association of the two variables, the closer the Pearson correlation coefficient r will be to either +1 or −1, depending on whether the relationship is positive or negative, respectively. A value of 0 indicates that there is no association between the two variables.

In the end, as a quantitative measure of the influence and relative importance of multiple drivers controlling HN, an analysis of variance (ANOVA) was conducted based on multiple linear regression models (Miller, 1997). In the linear model, the outcome was HN and the predictors were P, TMEAN, NAO and AO, considered as acting simultaneously. The analysis of the regression sum of squares (RSS) of each explanatory variable enabled calculating the explained variance of the concurrent drivers and therefore determining which of them explains better HN. Moreover, ANOVA provides the residuals, which is the variance not explained by individual predictors. The used sum-of-squares are of type I, which corresponds to a sequential analysis of variance.

3.5 | Code and data availability

All computations were performed with the statistical software R (version 4.0.2), using the RStudio interface version 1.1.463 (R Core Team, 2020). Some maps were produced using QGIS (version 2.18.13), a free Geographic Information System (GIS) software (QGIS Development Team, 2016). R scripts and the final revised database are openly available in Bozzoli (2022) and in GitHub (https://github.com/MBozzoli94/SnowTrendsAnalysis).

4 | RESULTS

This section presents first the HN climatology based on the collected observations, then the analysis of the monthly and seasonal trends of HN, HS, P and TMEAN. It follows the drivers correlation and attribution of HN to P, TMEAN, NAO and AO.

4.1 | Snowfall climatology

The average total seasonal (October–April) HN climatology for the region is illustrated in Figure 4a. The October–April period was chosen to maximize the availability of fresh snow data in the study region. The region exhibits a high variability, with a minimum of 19 cm in Riva del Garda at 65 m a.s.l. and a maximum of 588 cm in Passo Tonale at 1,880 m a.s.l., on the western border of the Trento province. Also, the year-to-year variability is very relevant for some stations, especially for low-elevation stations, where snowfall events are more sporadic (see Figures C1 and C2 of Appendix C).

It is interesting to notice that in the Adige Valley bottom, which is the main valley crossing the whole region from north to south, the average total seasonal HN is about 30 cm, with the maximum in the Trento area (40–44 cm) and the minimum in Rovereto (25 cm). Bolzano, on the other hand, with a slightly higher elevation with respect to Trento, presents an average seasonal value of 27 cm, due to a drier winter climate. Higher accumulations are recorded in the valleys in the upper part of the study area. Looking at the overall elevational distribution of HN (Figure 4b), it can be seen how the increase of seasonal HN with elevation is not linear, with a low increase up to about 750 m a.s.l. and a higher increase above. The more or less constant values up to 750 m a.s.l. are probably due to the development of cold pools in valleys, leading to a more uniform distribution of snowfall with elevation. Above 1,800 m a.s.l. the distribution becomes more dispersed, due to the larger variability of measured HN at high elevations (Figure 2a), as proved also by Blanchet *et al*. (2009).

4.2 | Snowfall trend analysis

The spatial distribution of the HN trends is highlighted in Figure 5, in connection with the individual months from October to April and for the entire snow season (Seas). HN trends in October are almost zero, except one in the northwestern part of the study area equal to +1.67 cm·decade^{-1}, but not significant. However, during this month most of the stations usually have not yet recorded any significant snowfall, hence, for this month, results are not easy to be interpreted. Also in November, most of the trends are close to zero (51/66), but nevertheless 14 positive trends are identified, most of them at altitudes higher than 1,500 m a.s.l.,

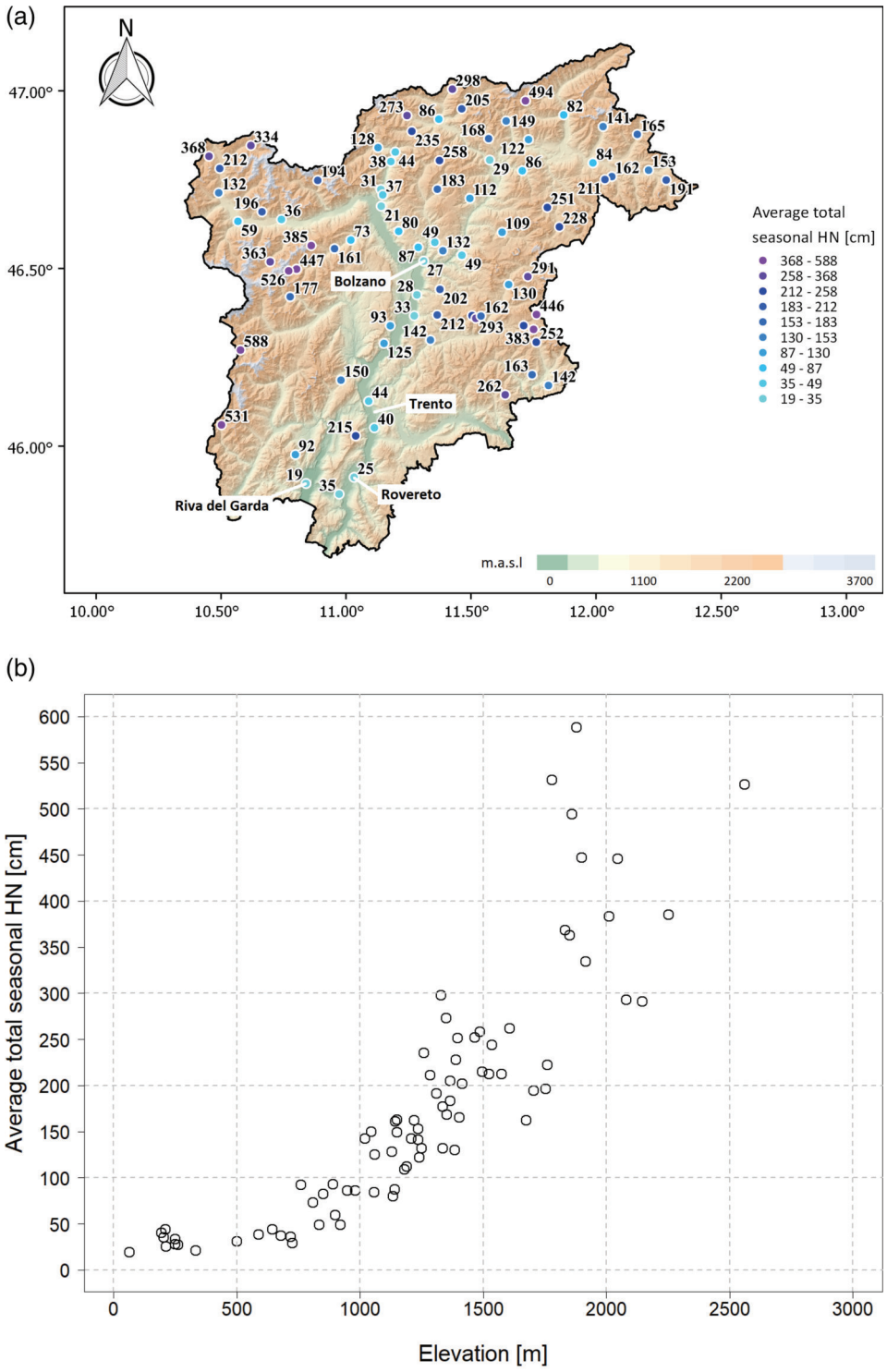

FIGURE 4 Spatial (a) and elevational (b) distribution of the average total seasonal HN over Trentino-South Tyrol in the period 1980–2020. Each point represents one station and the corresponding climatological value [Colour figure can be viewed at wileyonlinelibrary.com]

as shown in Figure 6, where the monthly trends are reported as a function of elevation. Only one trend in the northern part of the study region results to be negative and equals to −6.67 cm·decade^{-1}. December and April are the months with the largest fraction of negative trends. In December, 76% of the trends are negative (67/88), while in April the percentage of negative trends is 83% (54/65). The most negative absolute trends are observed at mid and high elevations, especially in April, when there is the strongest HN decrease and 62% of the trends are also statistically significant (Figure 6). In April the mean trends for (1000, 2000] and (2000, 3000] m are −5.1 and −12.9 cm·decade^{-1}, respectively, corresponding to relative losses of 19.2 and 14.6%·decade^{-1}, respectively (Table 1).

During the core of the winter season (January–March), both positive and negative trends are found. Most

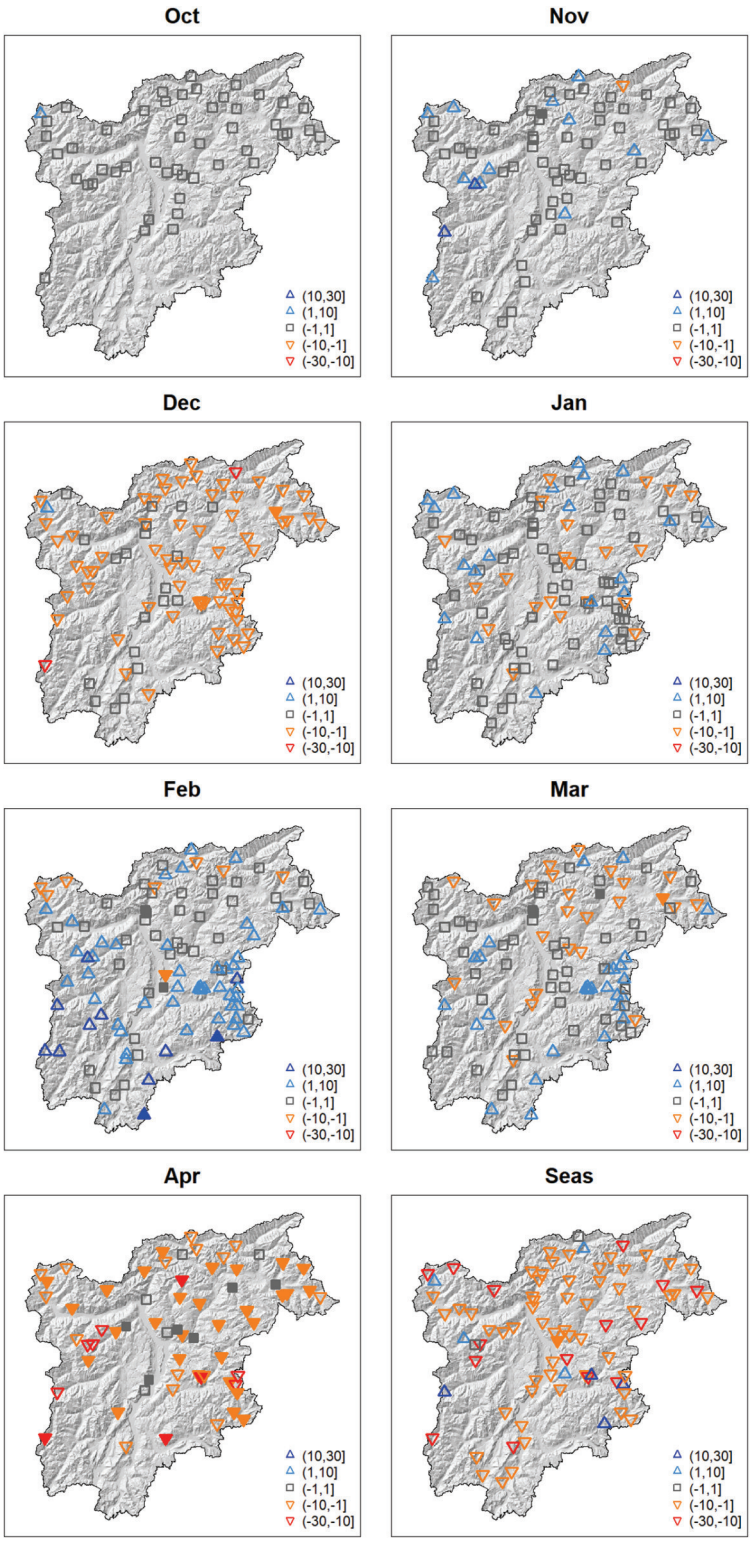

FIGURE 5 Spatial distribution of monthly (October–April) and seasonal snowfall (HN) trends expressed in cm·decade^{-1}. Each point represents one station and the corresponding trend value: blue (red) triangles indicate positive (negative) trends; grey squares indicate negligible trends (i.e., between −1 and 1). Full symbols indicate significant trends. Trentino-South Tyrol hill-shade is plotted in the background [Colour figure can be viewed at wileyonlinelibrary.com]

of them are not significant, though. In any case, they exhibit consistent spatial patterns (Figure 5). Most of the negative trends are found at low elevations, while positive trends occur mainly at high elevations (see also Figure 6). In particular, the southern part of the region at mid and high elevations exhibits increasing HN in February, with a maximum trend of +17.06 cm·decade^{-1} registered in the southeastern part of the region. However, these trends are statistically significant at two sites only (Figure 5). In February mean trends for the mid and high elevations are +3.9 and +7.5 cm·decade^{-1}, respectively, corresponding to a percentage increase of 7.1 and 10.9%·decade^{-1} (Table 1). For what concerns the low elevations, all trends are mostly

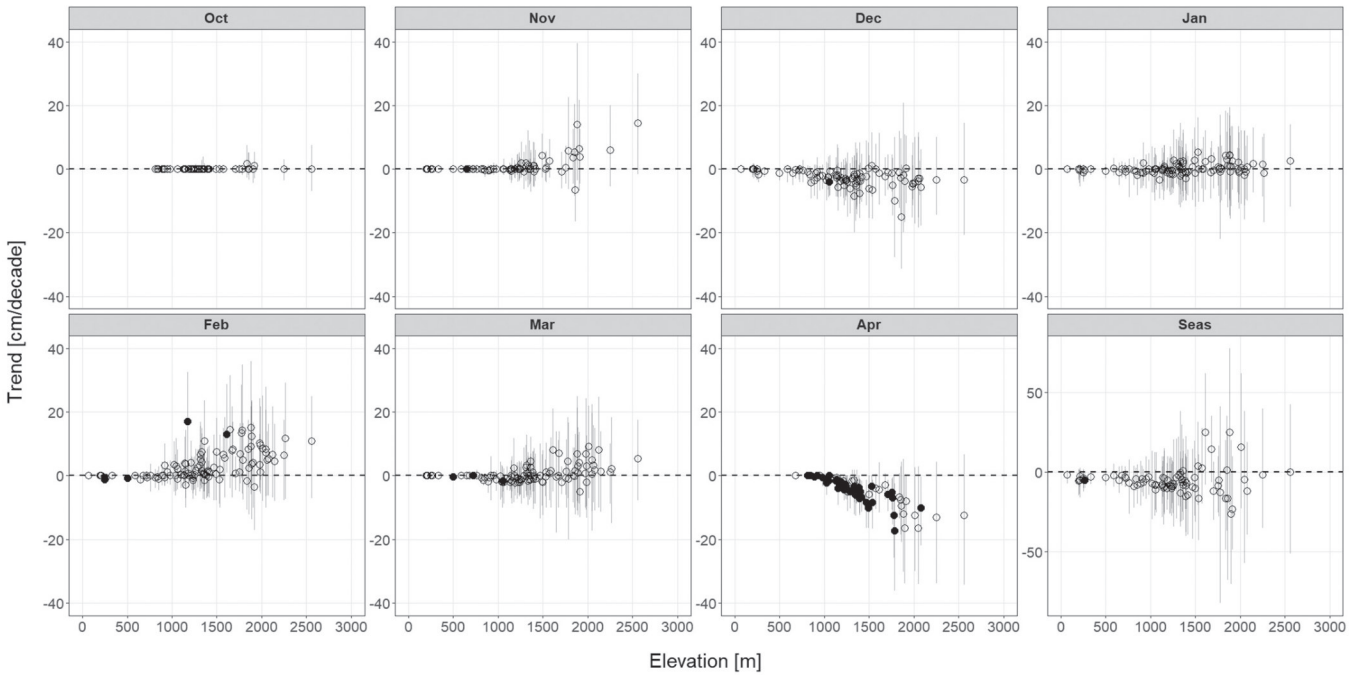

FIGURE 6 Monthly (October–April) and seasonal snowfall (HN) trends as function of elevation. Each point represents one station. Points with lines indicate the trend with the associated 95% confidence interval. Full dots indicate significant trends

negative (Figure 6) and the greatest loss is registered in December, with a mean trend of −1.0 cm·decade^{-1} (Table 1).

At the seasonal scale, trends are mainly negative, especially at low elevations, although at altitudes above 1,500 m a.s.l. eight positive trends are detected. However, at these elevations trends are affected by large uncertainty, as highlighted by the increase in the 95% confidence interval of the estimation (see *Seas* subplot in Figure 6). The increased uncertainty of the trends with elevation characterizes also the monthly time scale, as shown in all subplots of Figure 6. In addition, HN at these altitudes is very variable: years with high values alternate to others with much lower values, in contrast to low altitudes, where the average values are lower and more constant.

Overall, averaged seasonal trends are negative for all elevation ranges, as shown in the last row of Table 1. It is interesting to notice that in absolute terms the maximum negative trend of −6.4 cm·decade^{-1} is at intermediate elevations (1000, 2000] m, while in relative terms it is at the lowest elevations (0, 1000] m with −10.3%·decade^{-1}, due to the lower total seasonal accumulation. Instead, the highest elevations (2000, 3000] m exhibit much less negative trends, with a mean value of −0.5 cm·decade^{-1} (−0.3%).

4.3 | Snow depth trend analysis

The monthly and seasonal HN trends were compared with those of HS for the same gauging stations to evaluate their consistency. Trends for HS at monthly and seasonal time scales are reported in Figure 7 as function of elevation. In general, HS exhibits trends similar to those detected for HN, as it can be seen by visual comparison of Figure 6 with Figure 7. Also in this case, mid and low altitudes show negative trends, while at high altitudes, from January to March, some positive trends are present. However, there are some small differences, in particular during December and January. In December HS trends are less negative than the HN counterparts and in January at high elevations (above 2,000 m a.s.l.) HS trends are on average more positive. This behaviour is consistent with findings shown in Matiu *et al.* (2021), where mean positive HS trends are reported from November to January for the highest elevations (2000, 3000] m in the southern Alpine region. At seasonal level and below 2,000 m a.s.l., trends are negligible or slightly negative, while positive trends are found only in the two highest stations. This is confirmed also at monthly level, where the highest station always records positive trends and sometimes even statistically significant. As noticed for HN trends, also for HS mid and high elevation trends are characterized by large uncertainty. However, HS trends are less uncertain than those of HN, being HS a much more continuous variable through the winter with respect to HN.

4.4 | Precipitation and mean air temperature trend analysis

The precipitation (P) trends analysis indicates that the strongest signals are detected in November, when all

TABLE 1 Summary of monthly (October–April) and seasonal snowfall (HN) trends

	(0, 1000) m			(1000, 2000) m			(2000, 3000) m		
	#	AT	RT (%)	#	AT	RT (%)	#	AT	RT (%)
Oct	8	0.0	0.0	39	0.1	0.3	2	0.0	0.0
Nov	23	−0.1	−0.6	41	1.1	2.0	2	10.2	14.1
Dec	25	−1.0	−6.2	56	−3.5	−9.4	7	−3.8	−6.7
Jan	25	−0.4	−2.6	67	0.4	0.2	9	0.3	0.7
Feb	25	−0.1	−3.6	69	3.9	7.1	10	7.5	10.9
Mar	24	−0.3	−3.1	68	0.4	0.5	10	3.9	5.1
Apr	8	−0.1	−2.1	52	−5.1	−19.2	5	−12.9	−14.6
Seas	24	−4.5	−10.3	51	−6.4	−3.7	5	−0.5	−0.3

Note: For each elevation range the number of stations used for the calculation of the trend (#) and the mean value of the absolute (AT) and relative (RT) trends are indicated. AT are expressed in cm·decade^{-1}, and RT are expressed in %·decade^{-1}.

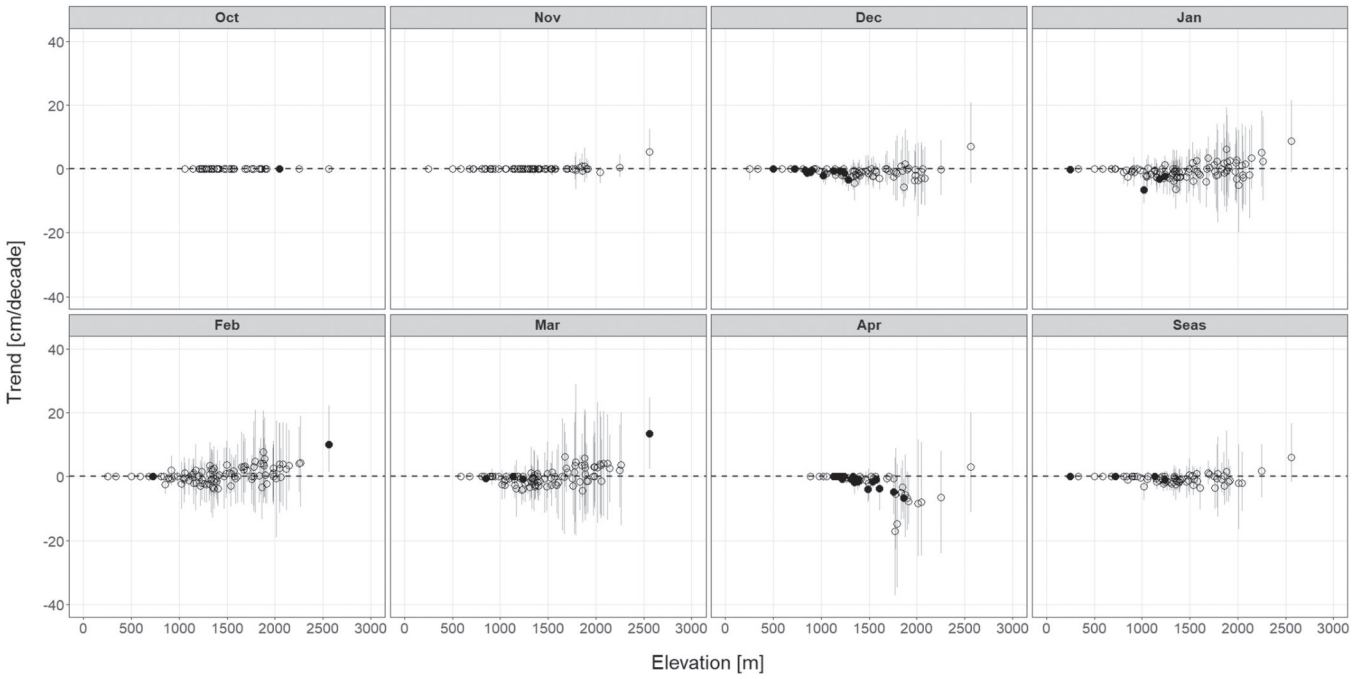

FIGURE 7 Monthly (October–April) and seasonal snow depth (HS) trends as function of elevation. Each point represents one station. Points with lines indicate the trend with the associated 95% confidence interval. Full dots indicate significant trends

trends are positive and many of them are also statistically significant (Figure 8). Most of the trends are in the range between 10 and 40 mm·decade^{-1}, with the maximum of 43.0 mm·decade^{-1} at Malga Bissina station (1,780 m a.s.l.), on the western border of Trentino. Some positive trends also occur in January, February and March, but they are not statistically significant. In the other months (October, December and April), trends are almost zero or slightly negative. However, on the aggregated seasonal scale, all trends are positive or strongly positive, but remain limited in relative terms (less than 4% mm·decade^{-1}). In fact, only in two stations statistically significant trends are detected. Remarkably, there is no evidence of elevation dependence in precipitation trends.

Trends analysis for TMEAN clearly shows that, except for January, trends are positive for each investigated elevation, with the largest trends detected at low elevations (Figure 9). The largest positive trends are recorded in April, all of them being statistically significant and in the range 0.5–1.0°C·decade^{-1}. On the contrary, the smallest trends are in January, with values above 1,500 m a.s.l. that are close to zero or slightly negative. However, none of the negative trends is statistically significant. From November to March, trends are dependent on elevation: strongly positive trends are found at low elevations, and

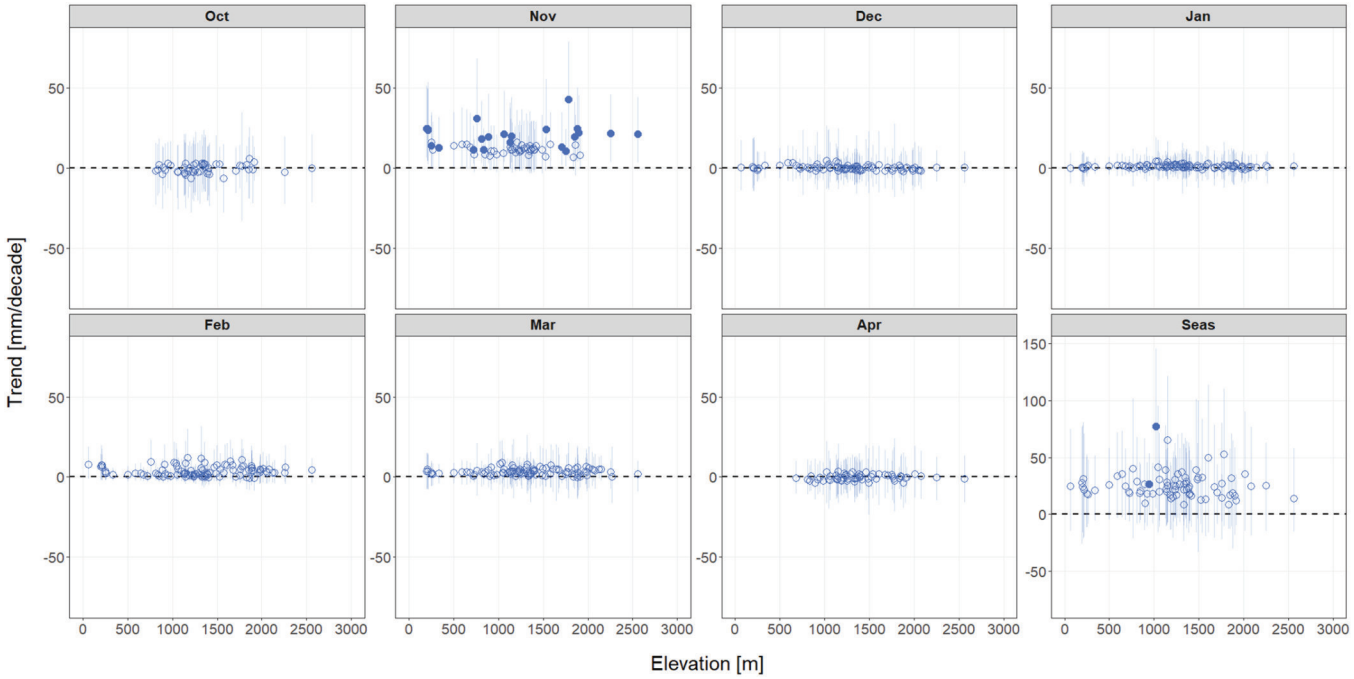

FIGURE 8 Monthly (October–April) and seasonal precipitation (P) trends as function of elevation. Each point represents one station. Points with lines indicate the trend with the associated 95% confidence interval. Full dots indicate significant trends [Colour figure can be viewed at wileyonlinelibrary.com]

less positive trends at high elevations. At seasonal scale, patterns of trends are similar to those computed in the individual months. Trends are all positive, especially at low elevations, and the majority of them are statistically significant, with values between 0.2 and 0.6°C·decade^{-1}.

4.5 | Correlation of HN with P, TMEAN, NAO and AO

Figure 10 shows the results of the correlation analysis between the HN time series and those of P, TMEAN, NAO and AO. The highest degree of correlation is between HN and P, especially above 1,000 m a.s.l. and during the period December–March. The occurrence of statistically significant values close to +1 indicates a strong positive correlation between HN and P, suggesting that, as precipitation increases, also snowfall increases. Indeed, this is consistent, considering that for those elevations and periods temperatures are low enough to guarantee solid precipitation (i.e., snowfall) in most of the cases. Concerning low-elevation sites, the highest degree of correlation is found between HN and TMEAN, especially in January and February. In this case the correlation is negative, and, as can be expected, the lower the mean temperatures, the higher the possibility of snowfall is. Again, the result is consistent, as temperatures are a limiting factor for snowfall at low altitudes. On the other hand, for mid and high elevations, negative correlation between HN and TMEAN is found in November, December, March and April. The correlation between HN and the teleconnection indices is rather weak. The only variable exhibiting relevant correlations is the AO index during December and January at low elevations. In these cases, favourable large-scale circulation patterns appear to be associated with snowfall. At seasonal level, it can be noted that for low elevations (below 1,000 m a.s.l.) the highest degree of correlation is between HN and TMEAN. Between 1,000 and 1,500 m a.s.l. the correlation with P and TMEAN is comparable, while above 1,500 m a.s.l. the strongest correlation is with P. The correlation with the teleconnection indices is less strong and often not significant, except for a few specific cases at low elevations.

4.6 | Attribution of HN to P, TMEAN, NAO and AO

In this section the attribution of HN variability to the predictors P, TMEAN, NAO and AO is discussed in terms of explained variance (EV). The results of the analysis of variance (ANOVA) are illustrated in Figure 11. At high elevations, P represents the driver that best explains HN, especially in January and February, when the fraction of HN variance explained by P is between 75 and 95%: this

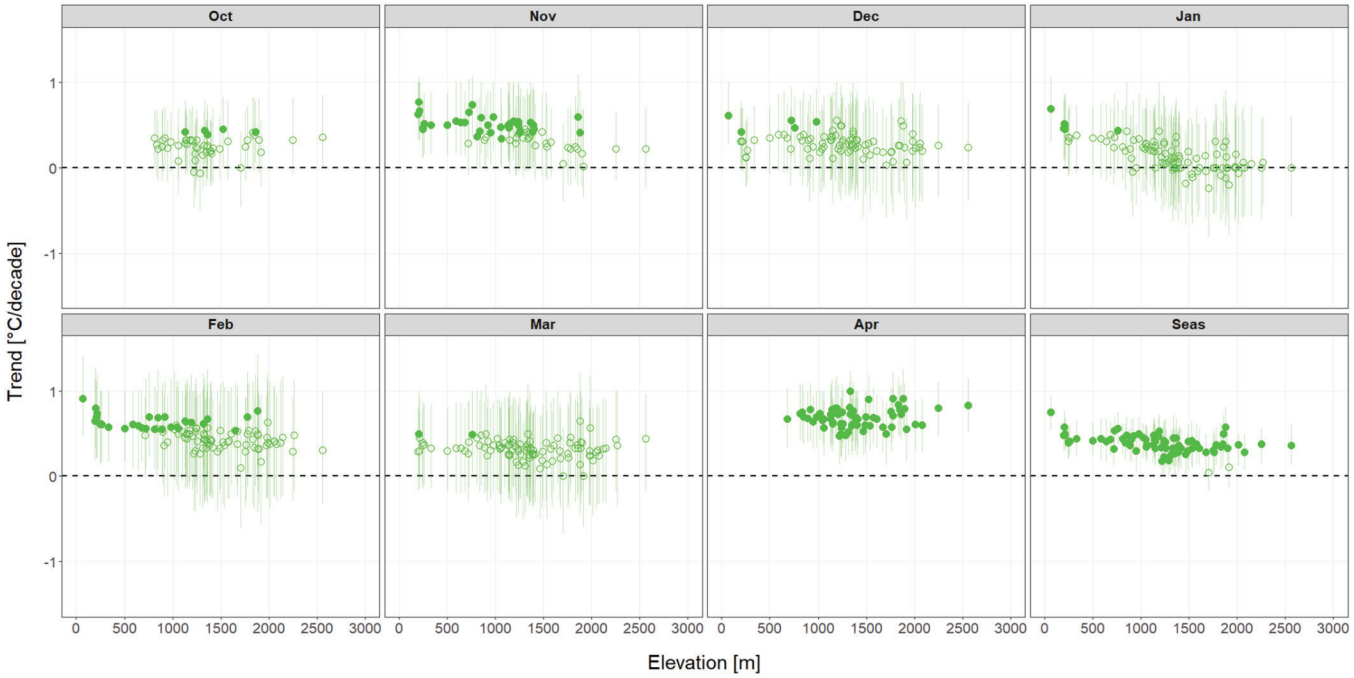

FIGURE 9 Monthly (October–April) and seasonal mean air temperature (TMEAN) trends as function of elevation. Each point represents one station. Points with lines indicate the trend with the associated 95% confidence interval. Full dots indicate significant trends [Colour figure can be viewed at wileyonlinelibrary.com]

suggests that during these 2 months at these altitudes most of the precipitation occurs as snow. Instead, at low elevations during January and February, TMEAN is the most important driver, since here temperatures are not always sufficiently low to allow for snowfall. This confirms the results presented above in terms of linear correlation analysis. On the other hand, TMEAN becomes more relevant for mid elevations during November and April, where the EV by TMEAN is 15–40% and 10–25%, respectively. In December and March at low elevations, P and TMEAN exhibit more or less the same fraction of EV, while at higher altitudes the variance is mostly explained by P, exceeding 75% in March. In October, the fraction of variance explained by each driver is very low (<25%), since in this month most of the stations have not yet recorded any significant snowfall, making the analysis not particularly meaningful, and quite difficult to interpret.

The contribution of NAO and AO is not relevant, except for specific months and at low elevations. More in detail, NAO presents non-negligible values of EV in October and March, while AO in November, December and February. The latter result is in agreement with that highlighted in the linear correlation analysis. Looking at the monthly unexplained variance (last column in Figure 11), it can be noticed that at low elevations HN can be explained only considering the simultaneous combination of all the drivers (residuals), while at mid–high elevations the variance explained by P is predominant. Also, at seasonal level, HN is mostly explained by the combination of all the drivers (see bottom-right subplot in Figure 11), with values between 50 and 75%. However, the EV of the single drivers is similar to that obtained at monthly scale: TMEAN is the best predictor below 1,000 m a.s.l., while P above 1,500 m a.s.l., confirming again the outcomes of the linear correlation analysis.

The above results can also be appreciated by analysing the spatial distribution of the driver presenting the highest EV for each considered time series (Figure 12). P is the predominant driver in explaining HN for the majority of the time series, especially at high elevations and from December to April. An exception is represented by the sites in the Adige Valley, which are the ones at the lowest elevations (<500 m a.s.l.), where in January and February TMEAN plays the most important role. In October and November the analysis shows uncertain results and the teleconnection indices also come into play. Finally, the analysis at seasonal level confirms that P prevails at high elevations while TMEAN at low elevations. The majority of the points is also statistically significant, suggesting the overall robustness of the attribution analysis.

5 | DISCUSSION

Altogether, our results show how seasonal trends are negative, especially at the lowest elevations, while some

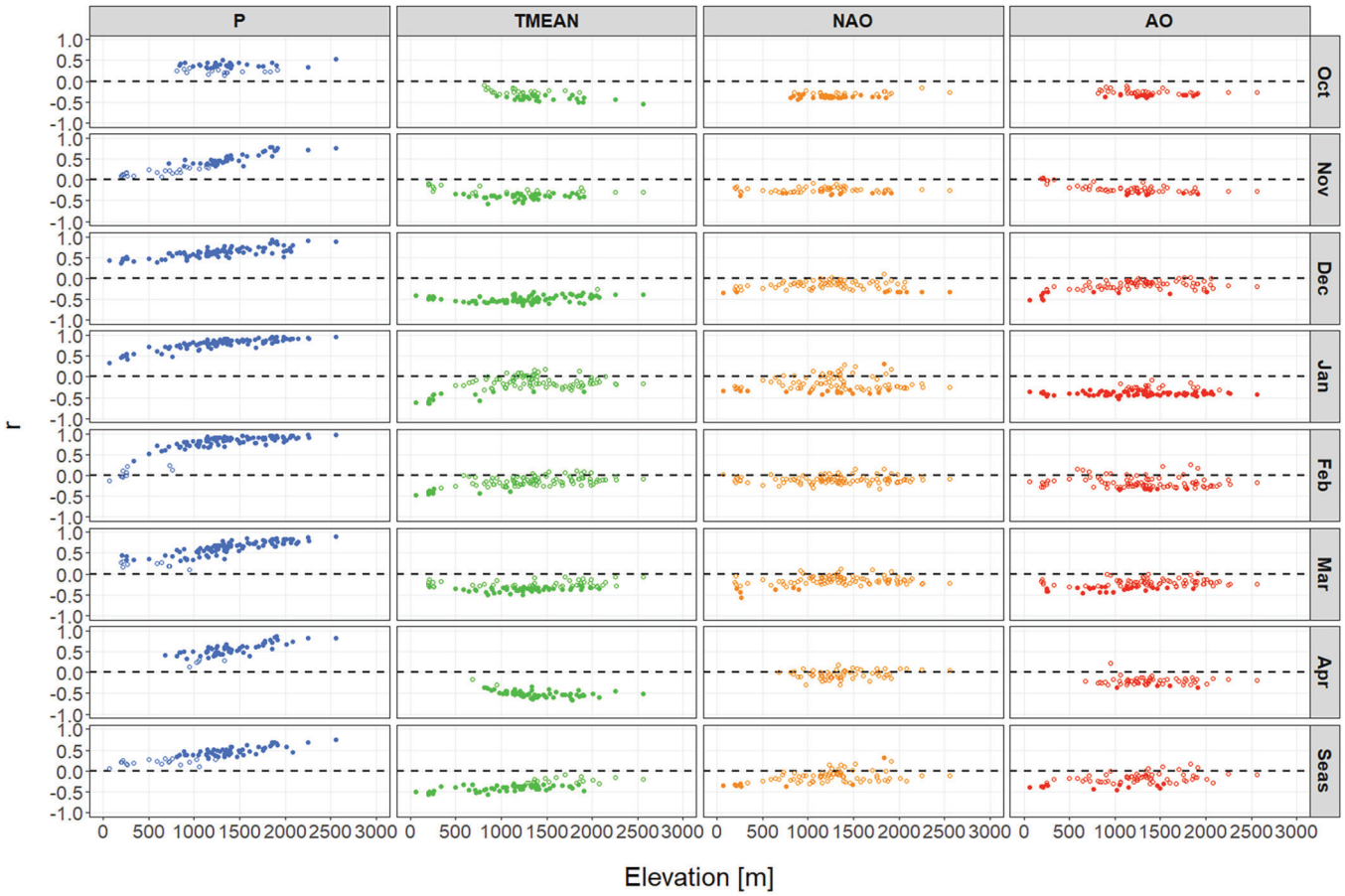

FIGURE 10 Correlation (r) between HN and P, TMEAN, NAO and AO, respectively, as function of elevation, evaluated at monthly and seasonal scale. Each point represents one station. Full dots indicate significant correlations [Colour figure can be viewed at wileyonlinelibrary.com]

positive trends have been found at the highest elevations. This result confirms the findings presented for extreme snowfall events simulated for the French Alps by Roux *et al.* (2021), who showed that the majority of trends are negative below 2,000 m a.s.l. and positive above that altitude. The dependence of snowfall trends on elevation highlighted in this work has been confirmed in other mountain chains, as found by Li *et al.* (2021) over the Tianshan Mountains, by Zhu *et al.* (2017) over the Qinghai-Tibet Plateau, and by Serquet *et al.* (2011), who reported a strong elevation dependence of the trends for snowfall/precipitation day ratio in Switzerland.

The results of the attribution analysis agree with Hammond *et al.* (2018), who presented global trends of snow persistence in the period 2001–2016. They showed how Europe at the latitude of the Alpine chain is one of the world's regions where the relative importance of temperature versus precipitation in controlling snow presence is strongly determined by the elevation. The general picture is therefore that at low elevations and mid-latitudes there are decreasing trends in snowfall and particularly in the snowfall/precipitation ratio (Safeeq *et al.*, 2016), while at high elevations or in cold/polar regions the decreasing trends are less evident. On the contrary, even some increasing trends are detected during the core of the winter season, when an increase in precipitation is found (Wang and He, 2013; Bjorkman *et al.*, 2015; Colucci *et al.*, 2021). The attribution analysis in our study highlights that decreasing HN trends at low altitudes are mainly explained by positive temperature trends, while increasing HN trends at higher elevations, found especially in the core winter months, are connected to positive trends in precipitation. Moreover, the combination of temperature and precipitation plays a relevant role in the warmer snow-season months, with a consequent earlier snow melt, confirming the findings by Knowles (2015) and Feng and Hu (2007) in the United States.

The attribution analysis also shows that the contribution of NAO and AO is not so relevant, except for specific months and at low elevations. This is in contrast with Beniston (1997) and Kim *et al.* (2013), who highlighted that periods with relative low snow amounts and duration are closely linked to the anomalies of the NAO index. However, Kim *et al.* (2013) proved that regional-scale

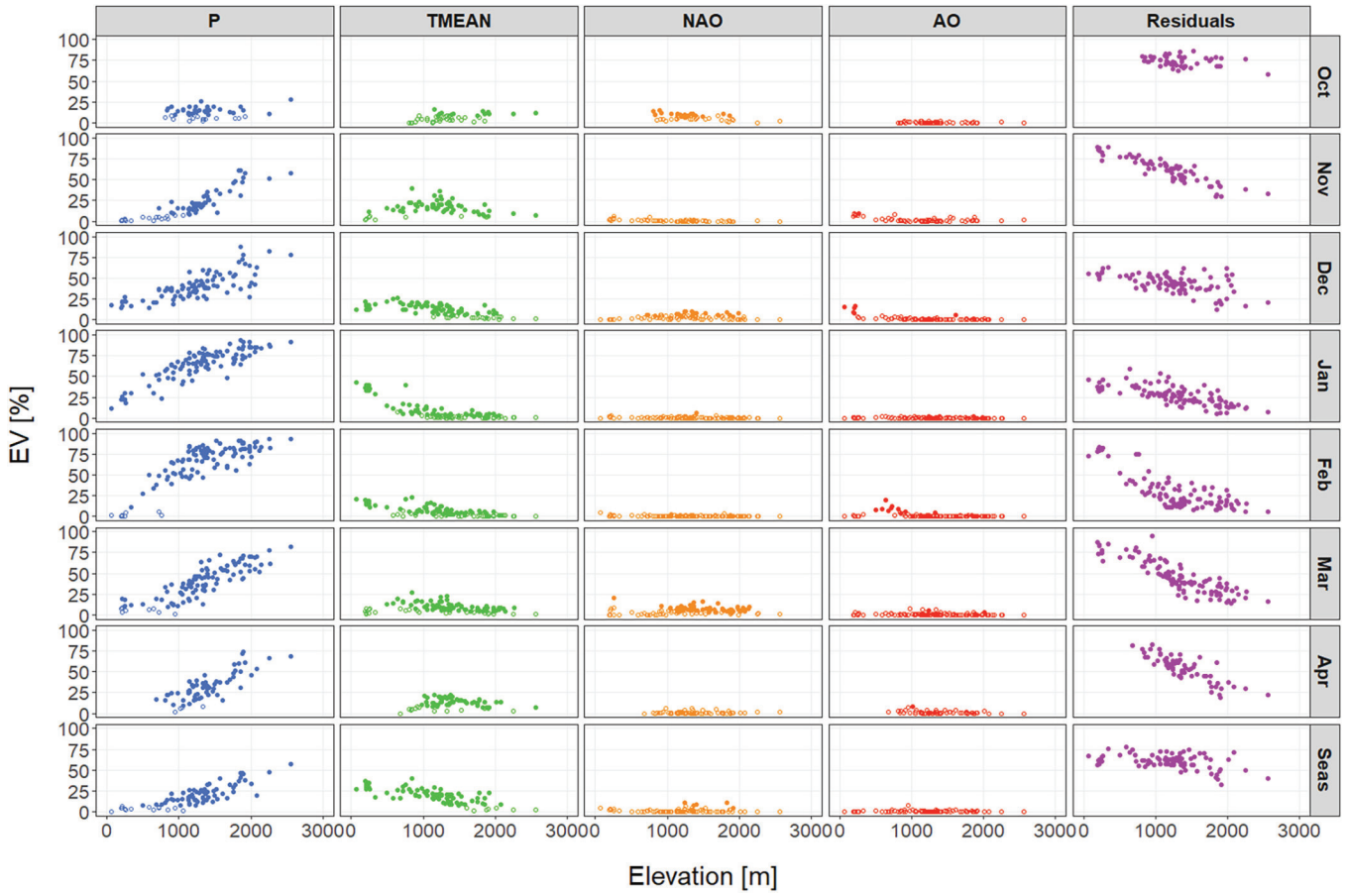

FIGURE 11 Fraction of explained variance (EV) in linear models of HN as function of P, TMEAN, NAO, AO at monthly and seasonal scale. Each point represents one model, that is one series. Full dots indicate significant values [Colour figure can be viewed at wileyonlinelibrary.com]

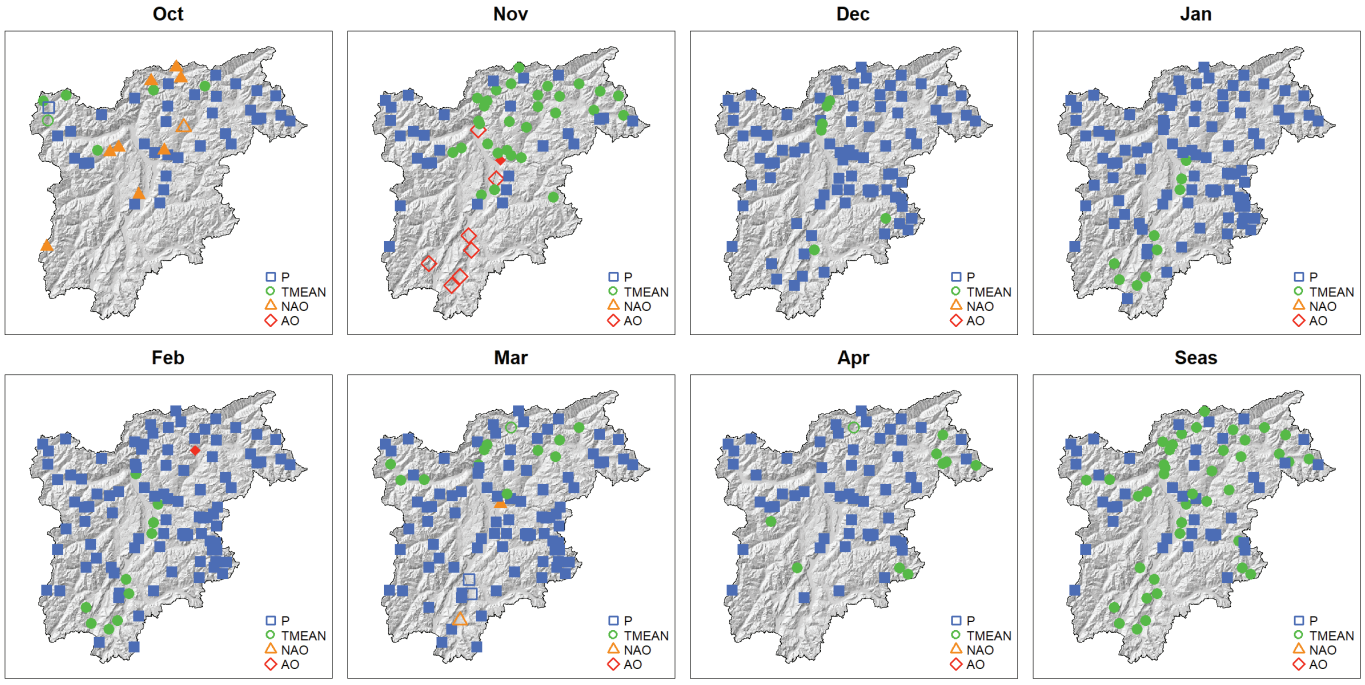

FIGURE 12 Spatial distribution of the driver with the highest explained variance for HN at monthly and seasonal scale. Filled symbols indicate significant values [Colour figure can be viewed at wileyonlinelibrary.com]

changes of winter snow cover vary significantly from one region to another. On the other hand, there is a good agreement of NAO and AO time series with the analysis of HN time series changing points presented in Figure 3. In fact, it shows a considerable number of negative changing points in the late 1980s/early 1990s, exactly when both NAO and AO registered a positive phase (see Figure D1 of Appendix D). In this condition, Hurrell (1995) proved that the polar cell becomes strongly compact, relegating cold air masses to high European latitudes, causing mild, dry winters in southern Europe. Those breakpoints were first described by Marty (2008) and later also demonstrated at the global level (Reid *et al*., 2016).

The analysis of changing points is coherent with the NAO and AO evolution also in the 2000s, when a consistent number of positive changing points are present, especially at high altitudes, and both NAO and AO show a neutral or slightly negative phase (Figure D1 of Appendix D). This negative phase might be associated to an unstable and cold atmospheric pattern over the southern sectors of Europe, which caused frequent precipitations, often in form of snowfall, during the winter seasons, leading to an increase in the average HN over the southern Europe (Hurrell and Van Loon, 1997; Trigo *et al*., 2002; Hurrell *et al*., 2003).

This negative phase ended in 2010, when the strongest negative value of the AO index was recorded (−4.27 in February 2010). Notice that during that year a temporary decrease in average European temperatures was registered (Cattiaux *et al*., 2010; Seager *et al*., 2010; Wang *et al*., 2010). In the most recent years a tendency toward a positive phase of both NAO and AO has been observed (Capozzi *et al*., 2021).

Looking at the overall elevation distribution of HN (Figure 4b), the cumulative HN vertical gradient appears to increase with elevation. Moreover, in the present case, Figure 4b shows that the average HN seasonal total is roughly constant up to 750 m a.s.l. A possible explanation is that in winter in the main valleys snowfall events at low elevations are often controlled by the occurrence of cold pools and associated ground-based thermal inversions, implying low vertical temperature gradients and therefore a more uniform distribution of snowfall with elevation. Moreover, the development of an isothermal layer with near-freezing temperatures is favoured in valleys by the cooling of the air due to melting precipitation (Unterstrasser and Zängl, 2006).

At the lowest elevations, as, for instance, in the valley floor of the Adige Valley, snowfall occurrence is becoming more occasional, in connection with the ongoing climate change. The current climatology shows an average total seasonal HN of about 30 cm, and trends are of about −4.5 cm·decade^{-1}. If these trends will be confirmed in the future, there could be a strong reduction in the seasonal snowfall, with a nearly null accumulation by 2090. This will have several impacts on natural systems and human society (Rydén, 2015).

At the highest elevations, where snow exerts a key hydrological, ecological and economic relevance, negative snowfall trends are weaker at the seasonal scale and even slightly positive in the core winter months, but strongly negative in spring. The consequences of these strongly negative trends in spring are already visible in the spring water availability and river regimes (Lutz *et al*., 2016; Diamantini *et al*., 2018; Mallucci *et al*., 2019). Instead, stable or positive trends in the core winter months could support winter tourism and ski industry.

6 | CONCLUSIONS

This study analysed 122 snowfall (HN) time series during the period 1980–2020 over a mountain region in the northeastern Italian Alps (Trentino-South Tyrol). To complement official monitoring networks and increase the data availability at lower elevations, amateur observations were included. After a preliminary quality check and a gap-filling procedure, HN trends were identified using the Sen's slope estimator and the Mann–Kendall trend test, and compared with precipitation (P) and mean air temperature (TMEAN) trends. Moreover, also large-scale predictors as the North Atlantic Oscillation (NAO) index and the Arctic Oscillation (AO) index were considered. A variance decomposition analysis was used to identify the drivers that better explain HN trends with respect to the month and the elevation.

HN trends were found to be strongly dependent on elevation, even if only in some cases they were statistically significant. Overall, the driver that best explains HN is the precipitation. However, for low elevations temperature assumes a more relevant role.

At seasonal scale, HN trends are mostly negative, especially at mid–low elevations, while at high elevations trends become more uncertain. In particular, in the core of the winter season (from January to March), positive HN trends were detected, especially for the mid–high elevations. HN trends in April are strongly negative and statistically significant. Considering three main elevation ranges, the following conclusions can be derived:

- (0–1000] m: the reduction of snowfall in this elevation range can be explained by the strong increase of TMEAN. P does not play a relevant role in explaining HN. In October and March, a certain contribution from

NAO is detected, while AO becomes more relevant in November, December and February.

- (1000–2000] m: this elevation range exhibits a strong variability. At the start and at the end of the winter season almost all the series recorded a reduction in snowfall, while during the core of the winter some of them recorded an increase of snowfall. Both P and TMEAN play a relevant role in explaining HN.
- (2000–3000] m: the slight increase of snowfall during the core of the winter season can be explained by a slight increase in P, given also that the mean air temperature in this elevation range is still sufficiently low to allow for snowfall in most cases. Therefore, P is the most important driver to explain HN.

At low elevations there is a clear decrease in HN due to a significant increase in the mean temperature. However, a relevant part of the variance was not explained by the considered predictors, suggesting a strong interannual variability. Suitable conditions for snowfall at low elevations are increasingly occasional and dependent on favourable large-scale atmospheric patterns. At high elevations, on the other hand, the slight increase in precipitation and the lower increase in the mean temperature, and, therefore, the presence of average temperatures still low enough to allow snowfall, favour the possibility to have an increase of HN in the core winter months. However, in spring, when temperatures are a limiting factor also at high elevations, HN trends are overall strongly negative.

Only few studies in the literature analysed HN time series. One reason might be the challenging task of quality checking the series. Our study is among the first ones performing a spatial consistency check of HN. While it was only applied at monthly scale, the method proved to be extremely useful in assessing the quality of the series and, for the future, it could enable more robust studies of HN in other areas. In the future, the analysis can be extended to higher temporal resolutions, such as weekly or daily values. The assessment of HN series and their trends adds valuable information to that derived from other snow-related parameters, such as HS, SCD or SWE. Altogether, an integrated analysis based on multiple snow-related variables can give a more comprehensive picture of snow cover changes. Additionally, high-quality and dense observation databases allow a better validation of physical model outputs or remote sensing products.

The presented snowfall climatology integrates and expands existing databases (Adler *et al.*, 2015; Matiu *et al.*, 2021) of a variable, HN, for which high quality and continuous records are difficult to find, especially at the lowest and highest elevations. However, in this work, thanks to the remarkable amount of 122 gauging stations distributed fairly uniformly over the study area, it was possible to attain a good spatial coverage across a large elevation gradient. In this study, official observations from institutional stations have been integrated with long-term time series from citizen observations. The availability of citizen weather stations has increased dramatically in recent years (Nipen *et al.*, 2019), representing an important resource which can integrate observational records coming from official networks. In particular, the inclusion of amateur (citizen science) time series of HN opens up new pathways for conducting snow cover research. The series passed all quality checks and can be considered of the same quality as series from meteorological offices. The procedure for measuring HN is rather straightforward, and the most stringent requirement for climatological analyses remains the completeness and length of available records. Passionate amateurs might perform rigorous measurements as fixed employees. Citizen science can thus represent a great potential to improve data coverage in space and time by providing observations for those locations not monitored by the official station networks, which is especially useful for variables, such as snowfall, that vary strongly over time and space. Citizen science could also involve different components of the society, for example school children, similarly to what has been proposed by Menzel *et al.* (2020) for analysing phenological observations. A benefit is that many find snowfall a fascinating topic, and fascination creates motivation, a key component of any scientific endeavour.

AUTHOR CONTRIBUTIONS

Giacomo Bertoldi: Scientific supervision; Conceptualization; formal analysis; investigation; writing – original draft; writing – review and editing. **Michele Bozzoli:** Conceptualization; data curation; formal analysis; investigation; software; validation; visualization; writing – original draft; writing – review and editing. **Alice Crespi:** Conceptualization; data curation; formal analysis; investigation; methodology; software; supervision; validation; writing – original draft; writing – review and editing. **Michael Matiu:** Conceptualization; data curation; formal analysis; methodology; software; supervision; validation; writing – original draft; writing – review and editing. **Lorenzo Giovannini:** Conceptualization; data curation; investigation; methodology; supervision; validation; writing – review and editing. **Dino Zardi:** Conceptualization; funding acquisition; methodology; project administration; supervision; writing – review and editing. **Bruno Majone:** Conceptualization; funding acquisition; investigation; methodology; project administration; resources; software; supervision; validation; writing – original draft; writing – review and editing.

ACKNOWLEDGEMENTS

We acknowledge for their support on data providing Walter Beozzo, Alberto Trenti, Mauro Gaddo (Meteotrentino and civil protection department of the Autonomous Province of Trento); Philipp Tartarotti, Rudi Nadalet, Roberto Dinale (Meteorology and avalanche prevention office of the Autonomous Province of Bolzano); Luca Fruner, Enrico Rizzi, Yuri Brugnara, Paolo Sartori, Matteo Calzà, Filippo Orlando, Oscar Filippini, Flavio Toni, Giacomo Poletti (Association Meteotrentinoaltoadige). This work has been partly supported by the projects funded by the Autonomous Province of Bozen/Bolzano – South Tyrol: "EcoHydro" (Eurac Research), "SnowTinel: Sentinel-1 SAR assisted catchment hydrology: toward an improved snow-melt dynamics for alpine regions" (Joint Project – Province of Bozen/Bolzano-Swiss National Foundation), and "SHE – Seasonal Hydrological-Econometric forecasting for hydropower optimization" (call "Research Südtirol/Alto Adige 2019") The authors thank the Department of Innovation, Research and University of the Autonomous Province of Bozen/Bolzano for covering the Open Access publications costs.

FUNDING INFORMATION

Eurac Research, Ecohydro Project; Department of Innovation, Research and University of the Autonomous Province of Bozen/Bolzano, SnowTinel and SHE projects.

CONFLICT OF INTEREST

The authors declare no potential conflict of interest.

ORCID

Giacomo Bertoldi https://orcid.org/0000-0003-0397-8103
Michele Bozzoli https://orcid.org/0000-0002-3844-0701
Alice Crespi https://orcid.org/0000-0003-4186-8474
Michael Matiu https://orcid.org/0000-0001-5289-0592
Lorenzo Giovannini https://orcid.org/0000-0003-1650-0344
Dino Zardi https://orcid.org/0000-0002-3573-3920
Bruno Majone https://orcid.org/0000-0003-3471-7408

REFERENCES

Adler, S., Chimani, B., Drechsel, S., Haslinger, K., Hiebl, J., Meyer, V., Resch, G., Rudolph, J., Vergeiner, J., Zingerle, C., Marigo, G., Fischer, A. and Seiser, B. (2015) Il clima del tirolo - alto adige - bellunese (Z. für Meteorologie und Geodynamik (ZAMG) - Ripartizione Protezione antincendi e civile (Provincia Autonoma di Bolzano) - Agenzia Regionale per la Prevenzione e Protezione Ambientale del Veneto (ARPAV), Ed.; D. C.-.S. T. (Bolzano), Trans.).

Anderson, E.A. (1976) *A Point Energy and Mass Balance Model of a Snow Cover*. Stanford, CA: Stanford University.

Bartolini, E., Claps, P. and D'Odorico, P. (2010) Connecting European snow cover variability with large scale atmospheric patterns. *Advances in Geosciences*, 26, 93–97.

Beaumet, J., Ménégoz, M., Morin, S., Gallée, H., Fettweis, X., Six, D., Vincent, C., Wilhelm, B. and Anquetin, S. (2021) Twentieth century temperature and snow cover changes in the French Alps. *Regional Environmental Change*, 21(4), 114. https://doi.org/10.1007/s10113-021-01830-x.

Beniston, M. (1997) Variations of snow depth and duration in the Swiss Alps over the last 50 years: links to changes in large-scale climatic forcings. In: *Climatic Change at High Elevation Sites*. Dordrecht: Springer, pp. 49–68.

Beniston, M., Farinotti, D., Stoffel, M., Andreassen, L.M., Coppola, E., Eckert, N., Fantini, A., Giacona, F., Hauck, C., Huss, M., Huwald, H., Lehning, M., López-Moreno, J.-I., Magnusson, J., Marty, C., Morán-Tejéda, E., Morin, S., Naaim, M., Provenzale, A., Rabatel, A., Six, D., Stötter, J., Strasser, U., Terzago, S., and Vincent, C. (2018) The European mountain cryosphere: a review of its current state, trends, and future challenges. *Cryosphere*, 12(2), 759–794. https://doi.org/10.5194/tc-12-759-2018.

Bjorkman, A.D., Elmendorf, S.C., Beamish, A.L., Vellend, M. and Henry, G.H.R. (2015) Contrasting effects of warming and increased snowfall on Arctic tundra plant phenology over the past two decades. *Global Change Biology*, 21(12), 4651–4661. https://doi.org/10.1111/gcb.13051.

Blanchet, J., Marty, C. and Lehning, M. (2009) Extreme value statistics of snowfall in the Swiss Alpine region. *Water Resources Research*, 45(5), W05424.

Bozzoli, M. (2022) Snow trends analysis v3.0. *Zenodo*. https://doi.org/10.5281/zenodo.6420941

Brunetti, M., Maugeri, M., Nanni, T., Auer, I., Bohm, R. and Schöner, W. (2006) Precipitation variability and changes in the Greater Alpine region over the 1800–2003 period. *Journal of Geophysical Research: Atmospheres*, 111(11), 1–29. https://doi.org/10.1029/2005jd006674.

Buchmann, M., Begert, M., Brönnimann, S. and Marty, C. (2021) Local-scale variability of seasonal mean and extreme values of in situ snow depth and snowfall measurements. *Cryosphere*, 15(10), 4625–4636.

Buchmann, M., Coll, J., Aschauer, J., Begert, M., Brönnimann, S., Chimani, B., Resch, G., Schöner, W. and Marty, C. (2022) Homogeneity assessment of Swiss snow depth series: comparison of break detection capabilities of (semi-) automatic homogenisation methods. *Cryosphere Discussions*, 16, 2147–2161.

Capozzi, V., De Vivo, C. and Budillon, G. (2021) Synoptic control over winter snowfall variability observed in a remote site of Apennine Mountains (Italy), 1884–2015. *Cryosphere Discussions*, 16, 1741–1763. https://doi.org/10.5194/tc-2021-363.

Cattiaux, J., Vautard, R., Cassou, C., Yiou, P., Masson-Delmotte, V. and Codron, F. (2010) Winter 2010 in europe: a cold extreme in a warming climate. *Geophysical Research Letters*, 37(20).

Chiogna, G., Majone, B., Paoli, K.C., Diamantini, E., Stella, E., Mallucci, S., Lencioni, V., Zandonai, F. and Bellin, A. (2016) A review of hydrological and chemical stressors in the adige catchment and its ecological status. *Science of the Total Environment*, 540, 429–443. https://doi.org/10.1016/j.scitotenv.2015.06.149.

Colucci, R.R., Žebre, M., Torma, C.Z., Glasser, N.F., Maset, E., Del Gobbo, C. and Pillon, S. (2021) Recent increases in winter snowfall provide resilience to very small glaciers in the Julian Alps, Europe. *Atmosphere*, 12(2), 263. https://doi.org/10.3390/atmos12020263.

Crespi, A., Matiu, M., Bertoldi, G., Petitta, M. and Zebisch, M. (2021) A high-resolution gridded dataset of daily temperature

and precipitation records (1980–2018) for Trentino-South Tyrol (north-eastern Italian Alps). *Earth System Science Data*, 13(6), 2801–2818. https://doi.org/10.5194/essd-13-2801-2021.

Danco, J.F., DeAngelis, A.M., Raney, B.K. and Broccoli, A.J. (2016) Effects of a warming climate on daily snowfall events in the Northern Hemisphere. *Journal of Climate*, 29(17), 6295–6318.

Di Marco, N., Avesani, D., Righetti, M., Zaramella, M., Majone, B. and Borga, M. (2021) Reducing hydrological modelling uncertainty by using modis snow cover data and a topography-based distribution function snowmelt model. *Journal of Hydrology*, 599, 126020. https://doi.org/10.1016/j.jhydrol.2021.126020.

Diamantini, E., Lutz, S.R., Mallucci, S., Majone, B., Merz, R. and Bellin, A. (2018) Driver detection of water quality trends in three large European river basins. *Science of the Total Environment*, 612, 49–62. https://doi.org/10.1016/j.scitotenv.2017.08.172.

Durand, Y., Giraud, G., Laternser, M., Etchevers, P., Mérindol, L. and Lesaffre, B. (2009) Reanalysis of 47 years of climate in the French Alps (1958–2005): climatology and trends for snow cover. *Journal of Applied Meteorology and Climatology*, 48(12), 2487–2512.

Endfield, G.H. and Morris, C. (2012) Exploring the role of the Amateur in the production and circulation of meteorological knowledge. *Climatic Change*, 113(1), 69–89.

Feng, S. and Hu, Q. (2007) Changes in winter snowfall/precipitation ratio in the contiguous United States. *Journal of Geophysical Research: Atmospheres*, 112(D15), D15109. https://doi.org/10.1029/2007jd008397.

Freedman, D., Pisani, R. and Purves, R. (2007) *Statistics (International Student Edition)*. New York: W. W. Norton.

Frei, P., Kotlarski, S., Liniger, M.A. and Schär, C. (2017) Future snowfall in the alps: projections based on the EURO-CORDEX regional climate models. *Cryosphere*, 12(1), 1–24. https://doi.org/10.5194/tc-12-1-2018.

Fugazza, D., Manara, V., Senese, A., Diolaiuti, G. and Maugeri, M. (2021) Snow cover variability in the Greater Alpine region in the MODIS era (2000–2019). *Remote Sensing*, 13(15), 2945. https://doi.org/10.3390/rs13152945.

Guo, L. and Li, L. (2015) Variation of the proportion of precipitation occurring as snow in the Tian Shan Mountains, China. *International Journal of Climatology*, 35(7), 1379–1393. https://doi.org/10.1002/joc.4063.

Haberkorn, A. (2019) European snow booklet—an inventory of snow measurements in Europe. *EnviDat*, 10. https://doi.org/10.16904/envidat.59.

Hammond, J.C., Saavedra, F.A. and Kampf, S.K. (2018) Global snow zone maps and trends in snow persistence 2001–2016. *International Journal of Climatology*, 38(12), 4369–4383. https://doi.org/10.1002/joc.5674.

Helfricht, K., Hartl, L., Koch, R., Marty, C. and Olefs, M. (2018) Obtaining sub-daily new snow density from automated measurements in high mountain regions. *Hydrology and Earth System Sciences*, 22(5), 2655–2668.

Hurrell, J.W. (1995) Decadal trends in the North Atlantic Oscillation: regional temperatures and precipitation. *Science*, 269(5224), 676–679.

Hurrell, J.W., Kushnir, Y., Ottersen, G. and Visbeck, M. (2003) An overview of the North Atlantic Oscillation. *Geophysical Monograph-American Geophysical Union*, 134, 1–36.

Hurrell, J.W. and Van Loon, H. (1997) Decadal variations in climate associated with the North Atlantic Oscillation. In: *Climatic Change at High Elevation Sites*. Dordrecht: Springer, pp. 69–94.

Huss, M., Bookhagen, B., Huggel, C., Jacobsen, D., Bradley, R.S., Clague, J.J., Vuille, M., Buytaert, W., Cayan, D.R., Greenwood, G., Mark, B.G., Milner, A.M., Weingartner, R. and Winder, M. (2017) Toward mountains without permanent snow and ice. *Earth's Future*, 5(5), 418–435. https://doi.org/10.1002/2016ef000514.

Jin, J. and Miller, N. (2007) Analysis of the impact of snow on daily weather variability in mountainous regions using MM5. *Journal of Hydrometeorology*, 8(2), 245–258.

Keller, F., Goyette, S. and Beniston, M. (2005) Sensitivity analysis of snow cover to climate change scenarios and their impact on plant habitats in alpine terrain. *Climatic Change*, 72(3), 299–319.

Kendall, M. (1975) *Rank Correlation Methods*. London: Griffin.

Kim, Y., Kim, K.-Y. and Kim, B.-M. (2013) Physical mechanisms of European winter snow cover variability and its relationship to the NAO. *Climate Dynamics*, 40(7), 1657–1669.

Knowles, N. (2015) Trends in snow cover and related quantities at weather stations in the conterminous United States. *Journal of Climate*, 28(19), 7518–7528. https://doi.org/10.1175/jcli-d-15-0051.1.

Kotlarski, S., Gobiet, A., Morin, S., Olefs, M., Rajczak, J. and Samacoïts, R. (2022) 21st century alpine climate change. *Climate Dynamics*, 60, 65–86. https://doi.org/10.1007/s00382-022-06303-3.

Kotlarski, S., Keuler, K., Christensen, O.B., Colette, A., Déqué, M., Gobiet, A., Goergen, K., Jacob, D., Lüthi, D., Van Meijgaard, E., Nikulin, G., Schär, C., Teichmann, C., Vautard, R., Warrach-Sagi, K., and Wulfmeyer, V. (2014) Regional climate modeling on European scales: a joint standard evaluation of the EURO-CORDEX RCM ensemble. *Geoscientific Model Development*, 7(4), 1297–1333.

Laiti, L., Mallucci, S., Piccolroaz, S., Bellin, A., Zardi, D., Fiori, A., Nikulin, G. and Majone, B. (2018) Testing the hydrological coherence of high-resolution gridded precipitation and temperature data sets. *Water Resources Research*, 54(3), 1999–2016. https://doi.org/10.1002/2017WR021633.

Leporati, E. and Mercalli, L. (1994) Snowfall series of Turin, 1784–1992: climatological analysis and action on structures. *Annals of Glaciology*, 19, 77–84.

Li, Q., Yang, T. and Li, L. (2021) Evaluation of snow depth and snow cover represented by multiple datasets over the Tianshan Mountains: remote sensing, reanalysis, and simulation. *International Journal of Climatology*, 42, 4223–4239. https://doi.org/10.1002/joc.7459.

Lin, W. and Chen, H. (2022) Changes in the spatial–temporal characteristics of daily snowfall events over the Eurasian continent from 1980 to 2019. *International Journal of Climatology*, 42(3), 1841–1853.

Lutz, S.R., Mallucci, S., Diamantini, E., Majone, B., Bellin, A. and Merz, R. (2016) Hydroclimatic and water quality trends across three Mediterranean river basins. *Science of the Total Environment*, 571, 1392–1406. https://doi.org/10.1016/j.scitotenv.2016.07.102.

Majone, B., Villa, F., Deidda, R. and Bellin, A. (2016) Impact of climate change and water use policies on hydropower potential in the south-eastern alpine region. *Science of the Total Environment*, 543, 965–980. https://doi.org/10.1016/j.scitotenv.2015.05.009.

Mallucci, S., Majone, B. and Bellin, A. (2019) Detection and attribution of hydrological changes in a large alpine river basin.

Journal of Hydrology, 575, 1214–1229. https://doi.org/10.1016/j.jhydrol.2019.06.020.

Mann, H. (1945) Nonparametric tests against trend. *Journal of the Econometric Society*, 13, 245–259.

Marcolini, G., Bellin, A., Disse, M. and Chiogna, G. (2017) Variability in snow depth time series in the adige catchment. *Journal of Hydrology*, 13, 240–254.

Marcolini, G., Koch, R., Chimani, B., Schöner, W., Bellin, A., Disse, M. and Chiogna, G. (2019) Evaluation of homogenization methods for seasonal snow depth data in the Austrian Alps, 1930–2010. *International Journal of Climatology*, 39(11), 4514–4530.

Marke, T., Hanzer, F., Olefs, M. and Strasser, U. (2018) Simulation of past changes in the Austrian snow cover 1948–2009. *Journal of Hydrometeorology*, 19(10), 1529–1545.

Marty, C. (2008) Regime shift of snow days in Switzerland. *Geophysical Research Letters*, 35(12), L12501. https://doi.org/10.1029/2008gl033998.

Marty, C. and Blanchet, J. (2012) Long-term changes in annual maximum snow depth and snowfall in Switzerland based on extreme value statistics. *Climatic Change*, 111(3), 705–721.

Marty, C., Tilg, A.-M. and Jonas, T. (2017) Recent evidence of large-scale receding snow water equivalents in the European alps. *Journal of Hydrometeorology*, 18(4), 1021–1031.

Mateus, C. (2021) Searching for historical meteorological observations on the Island of Ireland. *Weather*, 76(5), 160–165.

Matiu, M., Crespi, A., Bertoldi, G., Carmagnola, C. M., Marty, C., Morin, S., Schöner, W., Cat Berro, D., Chiogna, G., De Gregorio, L., Kotlarski, S., Majone, B., Resch, G., Terzago, S., Valt, M., Beozzo, W., Cianfarra, P., Gouttevin, I., Marcolini, G., Notarnicola, C., Petitta, M., Scherrer, S.C., Strasser, U., Winkler, M., Zebisch, M., Cicogna, A., Cremonini, R., Debernardi, A., Faletto, M., Gaddo, M., Giovannini, L., Mercalli, L., Soubeyroux, J.-M., Sušnik, A., Trenti, A., Urbani, S., and Weilguni, V. (2020) Snow cover in the European alps: station observations of snow depth and depth of snowfall. *Zenodo*. https://doi.org/10.5281/zenodo.4064129

Matiu, M., Crespi, A., Bertoldi, G., Carmagnola, C.M., Marty, C., Morin, S., Schöner, W., Cat Berro, D., Chiogna, G., De Gregorio, L., Kotlarski, S., Majone, B., Resch, G., Terzago, S., Valt, M., Beozzo, W., Cianfarra, P., Gouttevin, I., Marcolini, G., Notarnicola, C., Petitta, M., Scherrer, S. C., Strasser, U., Winkler, M., Zebisch, M., Cicogna, A., Cremonini, R., Debernardi, A., Faletto, M., Gaddo, M., Giovannini, L., Mercalli, L., Soubeyroux, J.-M., Sušnik, A., Trenti, A., Urbani, S., and Weilguni, V. (2021) Observed snow depth trends in the european alps: 1971 to 2019. *Cryosphere*, 15(3), 1343–1382. https://doi.org/10.5194/tc-15-1343-2021.

Menzel, A., Yuan, Y., Hamann, A., Ohl, U. and Matiu, M. (2020) Chilling and forcing from cut twigs—how to simplify phenological experiments for citizen science. *Frontiers in Plant Science*, 2020, 11. https://doi.org/10.3389/fpls.2020.561413.

Miller, R. (1997) *Beyond Anova: Basics of Applied Statistics*. Boca Raton, FL: CRC Press.

Mote, P.W., Li, S., Lettenmaier, D.P., Xiao, M. and Engel, R. (2018) Dramatic declines in snowpack in the western US. *npj Climate and Atmospheric Science*, 1(1), 1–6.

Nipen, T.N., Seierstad, I.A., Lussana, C., Kristiansen, J. and Hov, Ø. (2019) Adopting citizen observations in operational weather prediction. *Bulletin of the American Meteorological Society*, 101(1), 43–57. https://doi.org/10.1175/bams-d-18-0237.1.

Notarnicola, C. (2020) Hotspots of snow cover changes in global mountain regions over 2000–2018. *Remote Sensing of Environment*, 243, 111781. https://doi.org/10.1016/j.rse.2020.111781.

Olefs, M., Koch, R., Hiebl, J., Haslinger, K. and Schöner, W. (2017) Seasonal snow cover evolution in the nationalparks Austria since 1961. In: *6th Symposium for Research in Protected Areas*, pp. 475–478.

Olefs, M., Koch, R., Schöner, W. and Marke, T. (2020) Changes in snow depth, snow cover duration, and potential snowmaking conditions in Austria, 1961–2020—a model based approach. *Atmosphere*, 11(1), 7600. https://doi.org/10.3390/atmos11121330.

Pepin, N., Arnone, E., Gobiet, A., Haslinger, K., Kotlarski, S., Notarnicola, C., Palazzi, E., Seibert, P., Serafin, S., Schöner, W., Terzago, S., Thornton, J., Vuille, M. and Adler, C. (2022) Climate changes and their elevational patterns in the mountains of the world. *Reviews of Geophysics*, 60, e2020RG000730. https://doi.org/10.1029/2020rg000730.

Pettitt, A. (1979) Non parametric approach to the change point problem. *Applied Statistics*, 28, 126–135.

Pirazzini, R., Leppänen, L., Picard, G., Lopez-Moreno, J.I., Marty, C., Macelloni, G., Kontu, A., Von Lerber, A., Tanis, C. M., Schneebeli, M., De Rosnay, P., and Arslan, A.N. (2018) European in-situ snow measurements: practices and purposes. *Sensors*, 18(7), 2016. https://doi.org/10.3390/s18072016.

QGIS Development Team. (2016) *Qgis Geographic Information System*. Las Palmas: QGIS Association. Qgis version used: 2.18. Available at: https://www.qgis.org.

Quadrelli, R., Lazzeri, M., Cacciamani, C. and Tibaldi, S. (2001) Observed winter alpine precipitation variability and links with large-scale circulation patterns. *Climate Research*, 17(3), 275–284. https://doi.org/10.3354/cr017275.

R Core Team. (2020) *R: A Language and Environment for Statistical Computing*. Vienna: R Foundation for Statistical Computing. Available at: http://www.R-project.org.

Reid, P.C., Hari, R.E., Beaugrand, G., Livingstone, D.M., Marty, C., Straile, D., Barichivich, J., Goberville, E., Adrian, R., Aono, Y., Brown, R., Foster, J., Groisman, P., Hélaouët, P., Hsu, H.H., Kirby, R., Knight, J., Kraberg, A., Li, J., Lo, T.T., Myneni, R.B., North, R.P., Pounds, J.A., Sparks, T., Stübi, R., Tian, Y., Wiltshire, K.H., Xiao, D. and Zhu, Z. (2016) Global impacts of the 1980s regime shift. *Global Change Biology*, 22(2), 682–703.

Roux, E.L., Evin, G., Eckert, N., Blanchet, J. and Morin, S. (2021) Elevation-dependent trends in extreme snowfall in the french alps from 1959 to 2019. *Cryosphere*, 15(9), 4335–4356. https://doi.org/10.5194/tc-15-4335-2021.

Rydén, J. (2015) Is a white christmas becoming rarer in southern parts of Sweden? *Theoretical and Applied Climatology*, 121(1), 53–59.

Safeeq, M., Shukla, S., Arismendi, I., Grant, G.E., Lewis, S.L. and Nolin, A. (2016) Influence of winter season climate variability on snow–precipitation ratio in the western United States. *International Journal of Climatology*, 36(9), 3175–3190. https://doi.org/10.1002/joc.4545.

Scherrer, S.C., Wüthrich, C., Croci-Maspoli, M., Weingartner, R. and Appenzeller, C. (2013) Snow variability in the Swiss Alps 1864–2009. *International Journal of Climatology*, 33(15), 3162–3173.

Schöner, W., Koch, R., Matulla, C., Marty, C. and Tilg, A.-M. (2019) Spatiotemporal patterns of snow depth within the Swiss-Austrian Alps for the past half century (1961 to 2012) and linkages to climate change. *International Journal of Climatology*, 39(3), 1589–1603.

Seager, R., Kushnir, Y., Nakamura, J.A., Ting, M. and Naik, N. (2010) Northern Hemisphere winter snow anomalies: ENSO, NAO and the winter of 2009/10. *Geophysical Research Letters*, 37(14), L14703.

Sen, P.K. (1968) Estimates of the regression coefficient based on Kendall's tau. *Journal of the American Statistical Association*, 63(324), 1379–1389.

Serquet, G., Marty, C., Dulex, J.-P. and Rebetez, M. (2011) Seasonal trends and temperature dependence of the snowfall/precipitation day ratio in Switzerland. *Geophysical Research Letters*, 38(7), L07703. https://doi.org/10.1029/2011gl046976.

Terzago, S., Fratianni, S. and Cremonini, R. (2013) Winter precipitation in western Italian Alps (1926–2010). *Meteorology and Atmospheric Physics*, 119(3), 125–136.

Trigo, R.M., Osborn, T.J. and Corte-Real, J.M. (2002) The North Atlantic Oscillation influence on Europe: climate impacts and associated physical mechanisms. *Climate Research*, 20(1), 9–17.

Unterstrasser, S. and Zängl, G. (2006) Cooling by melting precipitation in alpine valleys: an idealized numerical modelling study. *Quarterly Journal of the Royal Meteorological Society*, 132, 1489–1508.

Valt, M. and Cianfarra, P. (2010) Recent snow cover variability in the Italian Alps. *Cold Regions Science and Technology*, 64(2), 146–157.

Vernay, M., Lafaysse, M., Monteiro, D., Hagenmuller, P., Nheili, R., Samacoïts, R., Verfaillie, D. and Morin, S. (2022) The S2M meteorological and snow cover reanalysis over the French mountainous areas: description and evaluation (1958–2021). *Earth System Science Data*, 14(4), 1707–1733. https://doi.org/10.5194/essd-14-1707-2022.

Wang, C., Liu, H. and Lee, S.-K. (2010) The record-breaking cold temperatures during the winter of 2009/2010 in the Northern Hemisphere. *Atmospheric Science Letters*, 11(3), 161–168.

Wang, H. and He, S. (2013) The increase of snowfall in northeast China after the mid-1980s. *Chinese Science Bulletin*, 58(12), 1350–1354. https://doi.org/10.1007/s11434-012-5508-1.

Wolters, D. and Brandsma, T. (2012) Estimating the urban heat island in residential areas in The Netherlands using observations by weather amateurs. *Journal of Applied Meteorology and Climatology*, 51(4), 711–721.

Ye, H. and Cohen, J. (2013) A shorter snowfall season associated with higher air temperatures over northern Eurasia. *Environmental Research Letters*, 8(1), 014052.

Ye, K., Messori, G., Chen, D. and Woollings, T. (2022) An NAO-dominated mode of atmospheric circulation drives large decadal changes in wintertime surface climate and snow mass over Eurasia. *Environmental Research Letters*, 17(4), 044025.

Zhu, X., Wu, T., Li, R., Wang, S., Hu, G., Wang, W., Qin, Y. and Yang, S. (2017) Characteristics of the ratios of snow, rain and sleet to precipitation on the Qinghai-Tibet plateau during 1961–2014. *Quaternary International*, 444, 137–150. https://doi.org/10.1016/j.quaint.2016.07.030.

How to cite this article: Bertoldi, G., Bozzoli, M., Crespi, A., Matiu, M., Giovannini, L., Zardi, D., & Majone, B. (2023). Diverging snowfall trends across months and elevation in the northeastern Italian Alps. *International Journal of Climatology*, *43*(6), 2794–2819. https://doi.org/10.1002/joc.8002

APPENDIX A: ERRORS DISTRIBUTION A

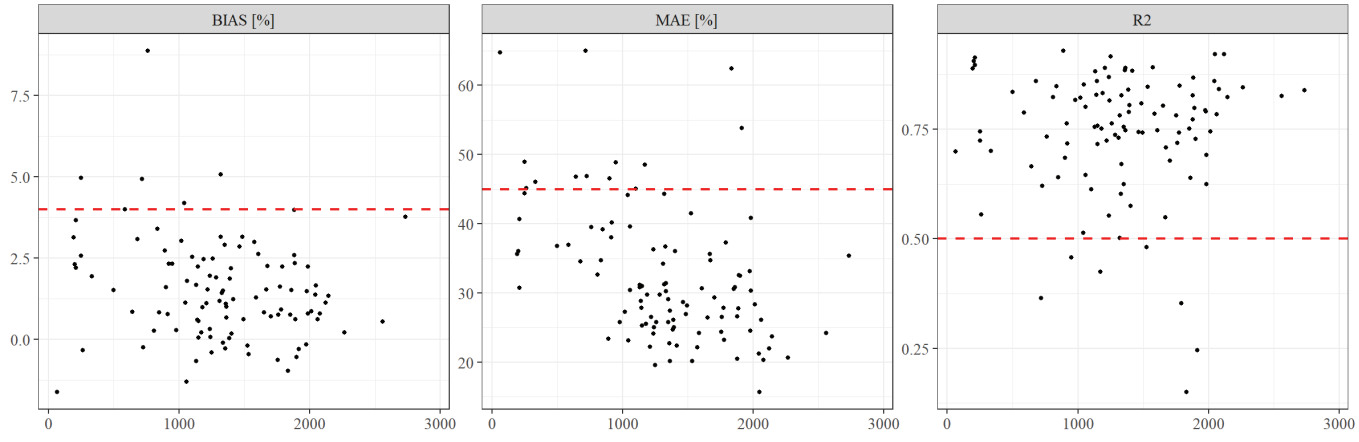

FIGURE A1 Errors distribution for observed and reconstructed time series: relative BIAS, relative MAE and R^2. Red dashed lines indicate thresholds of 4%, 45% and 0.5, respectively [Colour figure can be viewed at wileyonlinelibrary.com]

APPENDIX B: GAP FILLING AND TRENDS COMPARISON B

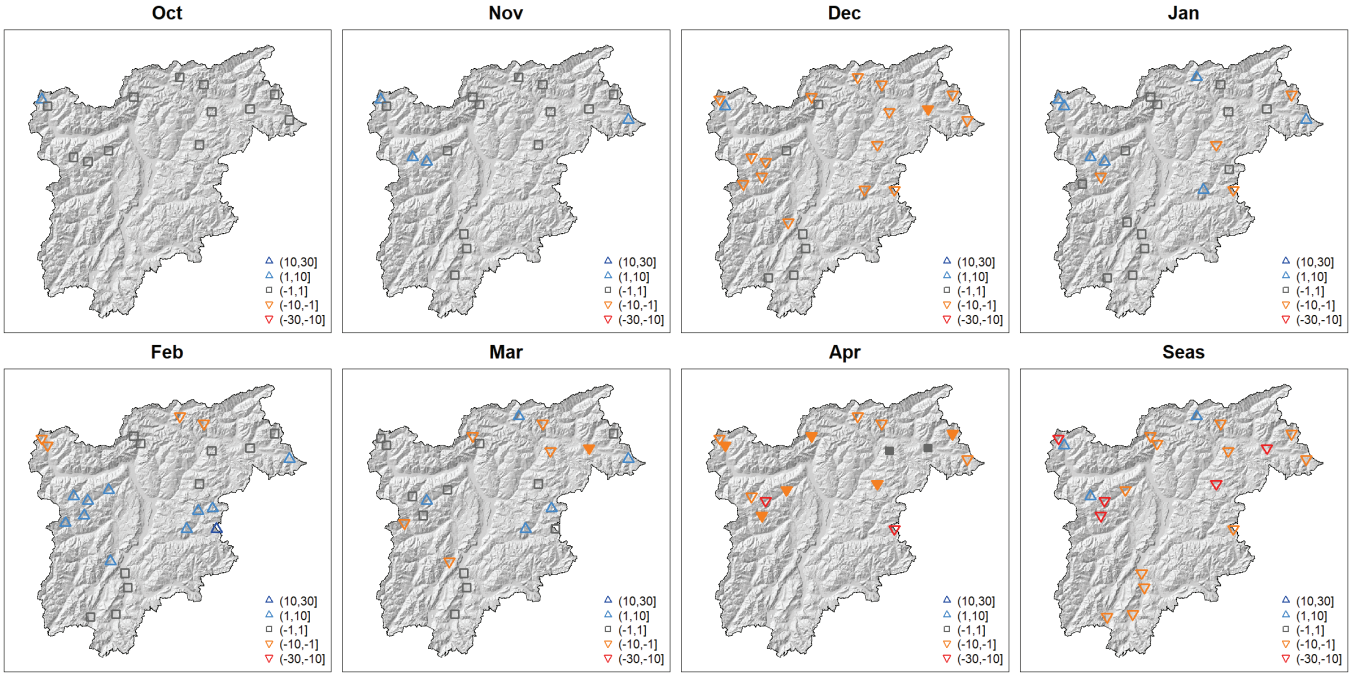

FIGURE B1 Spatial distribution of monthly (October–April) and seasonal snowfall (HN) trends expressed in cm·decade^{-1}. Each point represents one station and the corresponding trend value: blue (red) triangles indicate positive (negative) trends; grey squares indicate negligible trends (i.e., between −1 and 1). Full symbols indicate significant trends. Trentino-South Tyrol hill-shade is plotted in the background. Threshold imposed on the % of data gained after gap filling: 10% (trend case 1) [Colour figure can be viewed at wileyonlinelibrary.com]

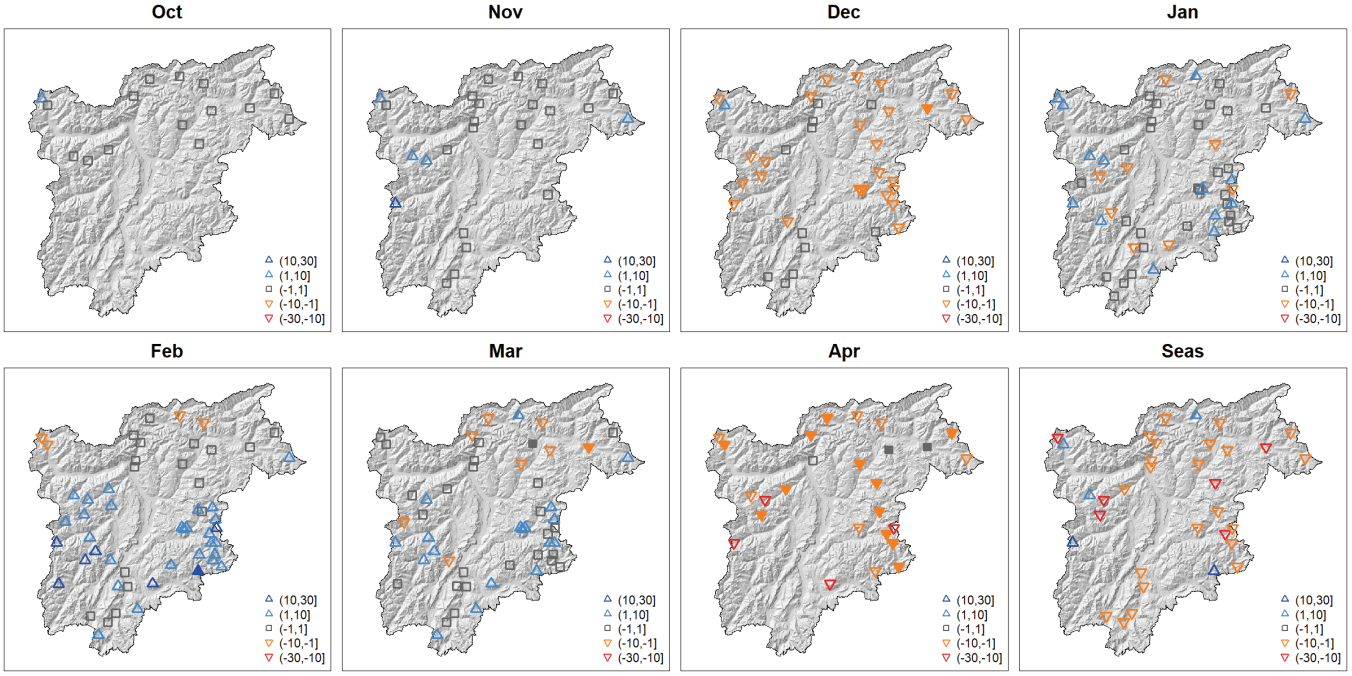

FIGURE B2 Same as Figure B1. Threshold imposed on the % of data gained after gap filling: 20% (trend case 2) [Colour figure can be viewed at wileyonlinelibrary.com]

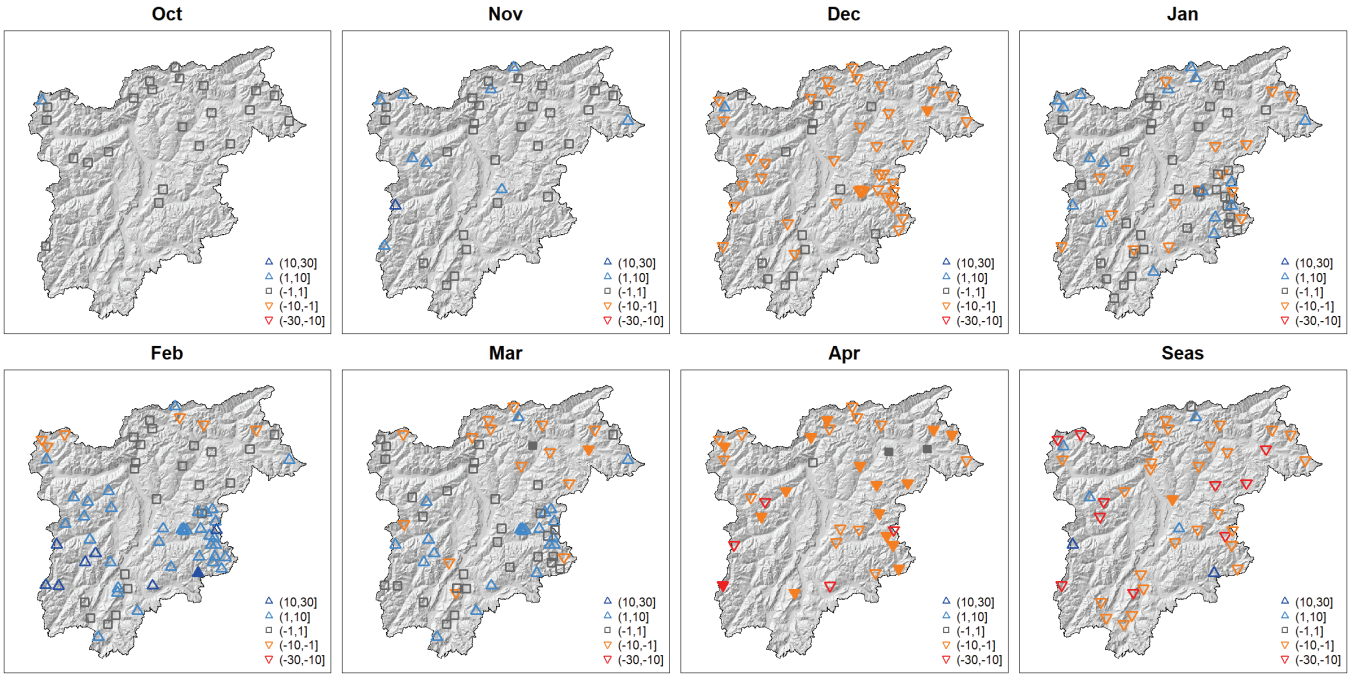

FIGURE B3 Same as Figure B1. Threshold imposed on the % of data gained after gap filling: 30% (trend case 3) [Colour figure can be viewed at wileyonlinelibrary.com]

TABLE B1 Comparison between trends calculated in the reference case and in the three test cases. Trend cases 1, 2, 3 represent the trends evaluated with the data set obtained considering only the time series with less than the 10, 20, 30% of data gained thanks to the gap filling procedure, respectively. For each case and elevation range the number of stations used for the the calculation of the trend (#) and the mean value of the absolute (AT) and relative (RT) trends are indicated. AT are expressed in cm·decade^{-1}, and RT are expressed in %·decade^{-1}

	(0, 1000) m			(1000, 2000) m			(2000, 3000) m		
	#	AT	RT (%)	#	AT	RT (%)	#	AT	RT (%)
Trend reference case	24	−4.5	−10.25	51	−6.36	−3.71	5	−0.51	−0.3
Trend case 1	6	−3.27	−8.83	12	−7.3	−4.25	1	−4.76	−1
Trend case 2	10	−3.35	−9.9	24	−4.04	−2.88	1	−4.76	−1
Trend case 3	12	−3.77	−10.42	34	−5.25	−3.24	3	−0.32	−0.33

APPENDIX C: SEASONAL SNOWFALL DATA C

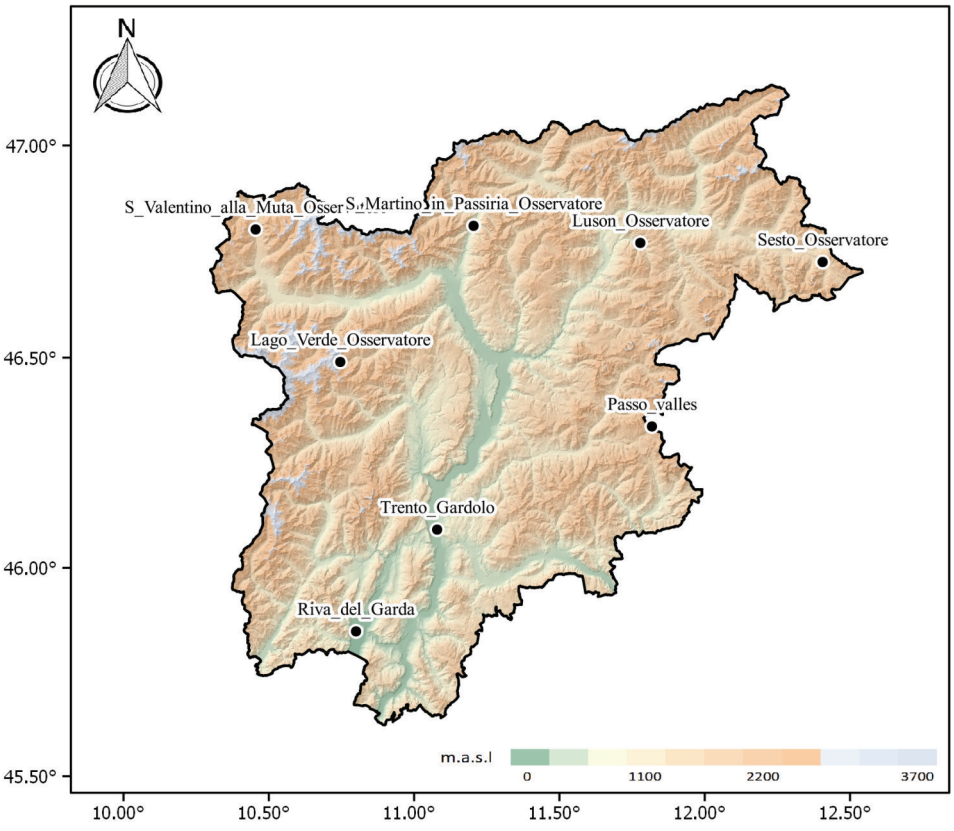

FIGURE C1 Location of the eight stations selected to show the seasonal snowfall variability [Colour figure can be viewed at wileyonlinelibrary.com]

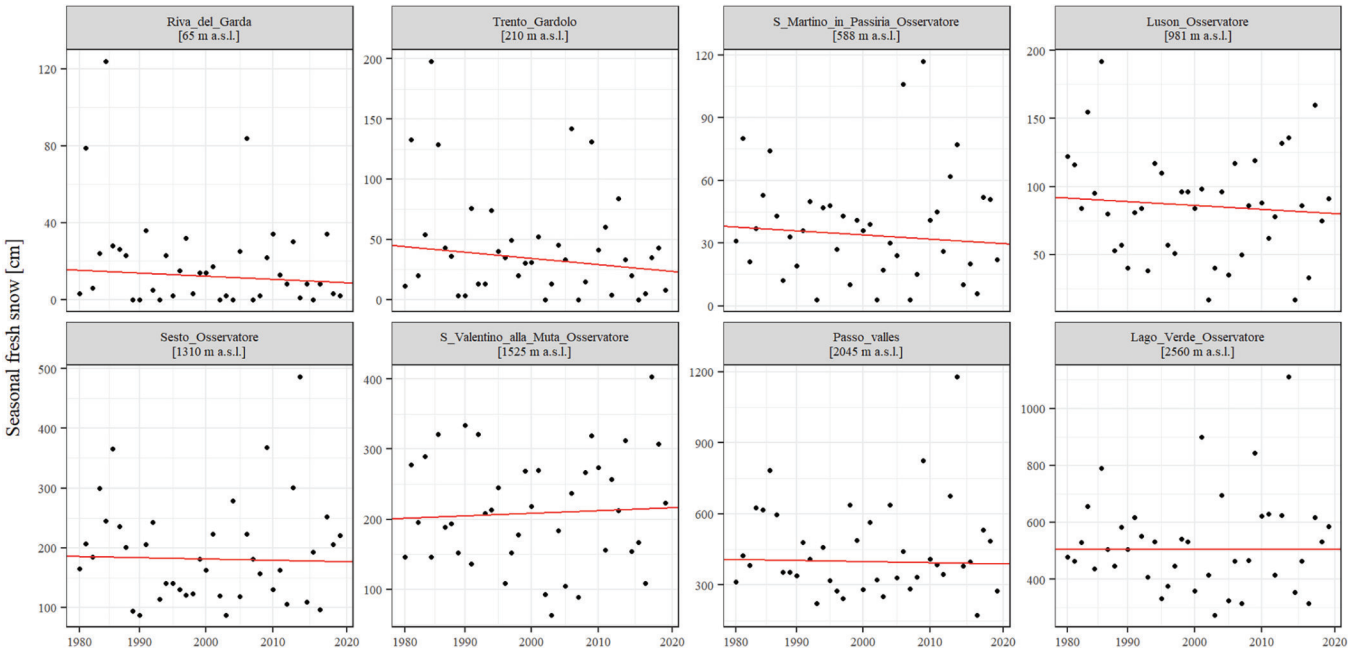

FIGURE C2 Seasonal snowfall time series of the eight stations selected to show the seasonal snowfall variability. Red lines indicate the trend [Colour figure can be viewed at wileyonlinelibrary.com]

APPENDIX D: NAO AND AO INDEX D

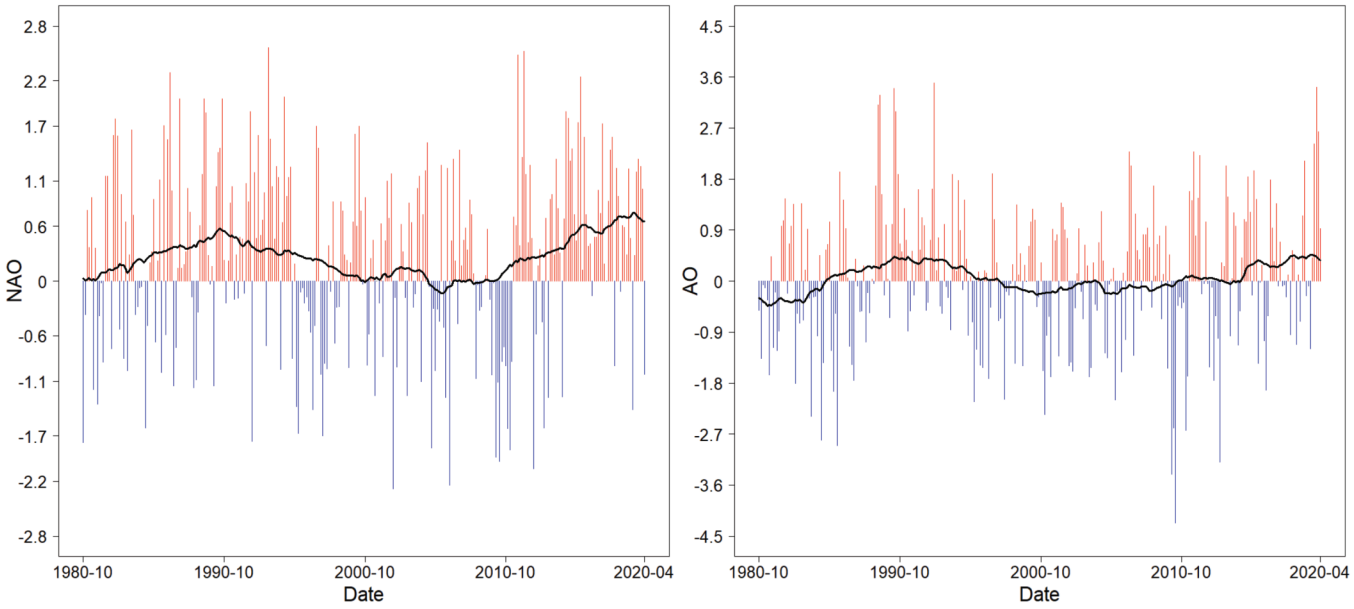

FIGURE D1 Monthly (October–April) NAO (a) and AO (b) time series during the period 1980–2020. The black line indicates the 10-year moving average [Colour figure can be viewed at wileyonlinelibrary.com]